

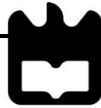
**Sara Joy Hawkins**

**ANÁLISE DO PROCESSO DE REGENERAÇÃO DO  
SISTEMA OLFATIVO DE UM ANFÍBIO**

**THE TIMING OF REGENERATION IN THE  
AMPHIBIAN OLFATORY SYSTEM**

## **DECLARAÇÃO**

Declaro que este relatório é integralmente da minha autoria, estando devidamente referenciadas as fontes e obras consultadas, bem como identificadas de modo claro as citações dessas obras. Não contém, por isso, qualquer tipo de plágio quer de textos publicados, qualquer que seja o meio dessa publicação, incluindo meios eletrônicos, quer de trabalhos acadêmicos.



**Sara Joy Hawkins**

**ANÁLISE DO PROCESSO DE REGENERAÇÃO DO  
SISTEMA OLFACTIVO DE UM ANFÍBIO**

**THE TIMING OF REGENERATION IN THE AMPHIBIAN  
OLFACTORY SYSTEM**

Dissertação apresentada à Universidade de Aveiro para cumprimento dos requisitos necessários à obtenção do grau de Mestre em Biologia Molecular e Celular, realizada sob a orientação científica da Professora Etelvina Maria de Almeida Paula Figueira, Professora Auxiliar do Departamento de Biologia da Universidade de Aveiro; e do Dr. Ivan Manzini, Líder do Grupo de Investigação do Centro de Microscopia em Nanoescala e Fisiologia Molecular do Cérebro (CNMPB – “Center for Nanoscale Microscopy and Molecular Physiology of the Brain”), da Universidade de Göttingen.

## **o júri**

presidente

**Prof. Maria Helena Abreu Silva**  
Professora Auxiliar do Departamento de Biologia da Universidade de Aveiro

arguente

**Prof. Sandra Isabel Moreira Pinto Vieira**  
Professora Auxiliar Convidada do Departamento de Ciências Médicas

orientadora

**Prof. Etelvina Maria de Almeida Paula Figueira**  
Professora Auxiliar do Departamento de Biologia da Universidade de Aveiro

## **agradecimentos**

O presente trabalho foi possível graças ao Dr. Ivan Manzini, que me proporcionou esta oportunidade única para trabalhar no seu laboratório e que se mostrou sempre disponível para me guiar ao longo do percurso de trabalho.

Queria agradecer toda a ajuda imprescindível proporcionada pelo restante grupo de trabalho: Post.Doc. Thomas Hassenklöver, pelo seu tempo e rigor na correção da minha dissertação; Ph.D. Thomas Offner, pelo seu excelente trabalho que contribuiu para os resultados obtidos; Ph.D. Kattarina Dittrich, pelas técnicas ensinadas e por acompanhar todo o meu trabalho laboratorial.

Queria agradecer também à Professora Etelvina Figueira, que possibilitou esta oportunidade de trabalhar na Alemanha. Obrigada pela ajuda, apoio e constante disponibilidade.

Finalmente queria agradecer à minha irmã Susana Grace Hawkins. Obrigada por me teres aturado e por seres a âncora que me mantém sã.

**palavras-chave**

Sistema olfativo periférico; Célula estaminal neuronal; Apoptose; Neuro-regeneração; *Xenopus laevis*

**resumo**

O estudo dos mecanismos responsáveis pela neuro-regeneração tem um marcado interesse para a compreensão dos princípios básicos que governam as interações celulares e moleculares no sistema nervoso, bem como um interesse clínico relevante. A limitada capacidade do sistema nervoso central para dar origem a novos neurónios é um obstáculo formidável para a recuperação do sistema após lesão neuronal ou doença neurodegenerativa. O sistema olfativo é um sistema ideal para o estudo do processo de recuperação após lesão neuronal, pois é conhecido no mundo científico pela sua capacidade contínua e vitalícia para repor células perdidas durante a renovação celular natural, bem como a sua notável capacidade para regenerar após uma lesão grave. O epitélio olfativo apresenta a capacidade para dar origem a novos neurónios ao longo de toda a vida. Neurónios sensoriais olfativos diferenciados são continuamente reintegrados num circuito já existente, mantendo assim o sentido do olfato. O objetivo desta tese é descrever as alterações morfológicas e funcionais que ocorrem ao longo do tempo no sistema olfativo de *Xenopus laevis* em estado larvar, após o corte do nervo olfativo. Os resultados obtidos através do uso de ensaios de imuno-histoquímica, bem como técnicas de marcação neuronal sensorial e de imagiologia de cálcio, indicam que a morte celular na população de neurónios sensoriais olfativos atinge o seu máximo 48 horas após a lesão, e que células estaminais encontradas na camada basal do epitélio olfativo são positivamente reguladas após lesão e proliferam rapidamente. Células de suporte parecem manter tanto a integridade morfológica como funcional após o corte do nervo olfativo. O epitélio olfativo recupera a sua estrutura morfológica inicial 1 semana após a lesão, momento em que os primeiros axónios atingem o bolbo olfativo e começam o processo de reintegração. Ocorre atividade espontânea das células mitrais/tufados do bolbo olfativo durante as primeiras semanas após a lesão, mas nenhuma atividade induzida por estímulo com odor foi observada. Depois de 3-4 semanas, atividade glomerular foi observada em alguns animais após a aplicação de estímulos, mas a resposta e morfologia glomerular foram claramente alteradas em relação ao controlo. Depois de 6-7 semanas as respostas parecem ter recuperado totalmente, indicando que o sistema olfativo de *X. laevis* em estado larvar recupera morfológica e funcionalmente 6-7 semanas após o corte do nervo olfativo.

**keywords**

Peripheral olfactory system; Neuronal stem cell; Apoptosis; Neuroregeneration; *Xenopus laevis*

**abstract**

Comprehending the mechanisms that make lifelong neurogenesis possible has a clear interest for the better understanding of the basic principles that govern cellular and molecular interactions in the nervous system, as well as a relevant clinical interest. The limited ability of the central nervous system to generate new neurons in order to replace those that have been lost is a formidable obstacle to recovery from neuronal damage caused by injury or neurodegenerative disease. The olfactory system (OS) is an ideal system to study the process of neuronal recovery after injury, as it is known for its lifelong capacity to replenish cells lost during natural turnover, as well as its remarkable ability to regenerate after severe lesion. The olfactory epithelium (OE) shows neurogenesis throughout life. Newly differentiated olfactory receptor neurons (ORNs) are continuously reintegrated into an existing circuitry to maintain the sense of smell. The aim of this thesis is to describe the morphological and functional alterations that occur over time in the OS of larval *Xenopus laevis*, after transection of the olfactory nerve (ON). Results obtained using immunohistochemistry essays, as well as sensory neuron labeling and calcium imaging techniques, indicate that ORN cell death reaches its peak 48 hours after transection, and that proliferating stem cells found in the basal cell layer of the OE are quickly upregulated after lesion. Supporting cells seem to maintain both morphological and functional integrity after transection of the ON. The OE recovers its original morphological structure 1 week after transection, at which time the first axons reach the olfactory bulb (OB) and begin the process of re-innervation. Spontaneous activity of mitral/tufted cells occurs in the OB during the first weeks after transection but no odor-induced activity is observed. After 3-4 weeks glomerular responses were observed in some animals upon application of stimulus, but the response and glomerular morphology are clearly altered as compared to control. After 6-7 weeks responses seem to have fully recovered, indicating that the OS of larval *X. laevis* recovers morphologically and functionally 6-7 weeks after ON transection.

# TABLE OF CONTENTS

LIST OF ABBREVIATIONS .....	2
LIST OF FIGURES.....	4
1. INTRODUCTION.....	5
1.1. Basics of vertebrate olfaction.....	6
1.2. Olfaction in larval <i>Xenopus laevis</i> .....	8
1.3. Regenerative capacity of the olfactory system.....	13
2. AIM OF THE MASTER THESIS .....	18
3. MATERIAL AND METHODS .....	20
3.1. Animal selection and determination of ontogenetic stages .....	20
3.2. Labeling of sensory neurons by olfactory nerve tracing and immunohistochemistry essays .....	20
3.3. Calcium imaging in the olfactory epithelium.....	22
3.4. Survey of olfactory sensory neuron re-innervation and olfactory bulb morphology ..	23
3.5. Calcium imaging in the olfactory bulb.....	24
3.5.1. Whole olfactory system preparation.....	24
3.5.2. Multiple cell bulk loading .....	25
3.5.3. Fast multiphoton calcium imaging in the olfactory bulb.....	25
3.5.4. Analysis of calcium imaging data and reactive volume generation .....	26
4. RESULTS .....	27
4.1. Changes in the olfactory epithelium after olfactory nerve transection.....	27
4.1.1. Apoptotic events.....	28
4.1.2. Proliferative activity .....	29
4.1.3. Morphological integrity of supporting cells .....	29
4.2. Calcium imaging in the olfactory epithelium.....	30
4.3. Changes in the olfactory bulb after olfactory nerve transection.....	33
4.3.1. Morphological changes (axonal rewiring) .....	33
4.3.2. Functional changes (cellular and glomerular responses).....	34
5. DISCUSSION .....	37
5.1. Olfactory receptor neuron cell death and basal cell proliferation are tightly coupled and highly regulated .....	39
5.2. Olfactory nerve transection does not eliminate supporting and basal cell function	41
5.3. Glomerular responses are lost after olfactory nerve transection, and recover after 6-7 weeks.....	44
REFERENCES.....	47



## LIST OF ABBREVIATIONS

OS	olfactory system
OE	olfactory epithelium
ON	olfactory nerve
CNS	central nervous system
OB	olfactory bulb
ORN	olfactory receptor neuron
BC	basal cell
SC	supporting cell
cAMP	cyclic adenosine monophosphate
BCL	basal cell layer
BrdU	bromo-2'-deoxyuridine
DAPI	4,6-diamidino-2-phenylindole
LP	lamina propria
ORN <sub>L</sub>	olfactory receptor neuron layer
PC	principal cavity
SCL	supporting cell layer
AOB	accessory olfactory bulb
[Ca <sup>2+</sup> ] <sub>i</sub>	intracellular calcium concentration
OO	olfactory organ
IC	intermediate cluster
MC	medial cluster

LC	lateral cluster
VNO	vomeronasal organ
PGC	periglomerular cell
OEC	ensheathing cell
MS-222	ethyl 3-aminobenzoate methanesulfonate
HPLC	high-performance liquid chromatography
PBS	phosphate buffered saline
PBST	PBS with Triton X-100 (detergent)
NGS	normal goat serum
KLH	keyhole limpet hemocyanin
LSM	laser scanning confocal microscope
DMSO	dimethyl sulfoxide

## LIST OF FIGURES

**Figure 1** - Location of the stem cell niche within the olfactory epithelium of larval *Xenopus laevis*.

**Figure 2** - Olfactory system of larval *Xenopus laevis*, highlighting the organization of the glomerular clusters in the olfactory bulb.

**Figure 3** - Schematic drawing of a section through the olfactory epithelium and the olfactory bulb in the normal olfactory system of larval *Xenopus laevis*.

**Figure 4** - Schematic representation of the experimental approach.

**Figure 5** – Changes in the olfactory epithelium: Biocytin backfill coupled to active caspase-3 staining, at different time points after transection of the olfactory nerve.

**Figure 6** - Changes in the olfactory epithelium: Biocytin backfill coupled to BrdU staining, at different time points after transection of the olfactory nerve.

**Figure 7** - Changes in the olfactory epithelium: Biocytin backfill coupled to cytokeratin staining, at different time points after transection of the olfactory nerve.

**Figure 8** - Functional calcium imaging performed on acute slices of the olfactory epithelium shows transection does not eliminate supporting or basal cell responses.

**Figure 9** - Changes in olfactory bulb connectivity after olfactory nerve transection.

**Figure 10** - Reestablishment of olfactory bulb connectivity after olfactory nerve transection.

**Figure 11** - Loss and recovery of response in the olfactory bulb after olfactory nerve transection.

**Figure 12** - Olfactory system regains structural and functional integrity over the course of 7 weeks after transection of the olfactory nerve.

# 1. INTRODUCTION

Although many tissues are able to regenerate their characteristic cell types throughout life, this does not seem to be the case in the central nervous system (CNS). Once development is complete, most stem cells in the CNS undergo terminal differentiation and no longer divide (Kauffman, 1968; Caviness et al., 1995). However, neuronal stem cell populations have been found to persist after development is terminated in restricted niches of the CNS. These constitutively active neurogenic zones include the subventricular and subgranular zone (Altman and Das, 1965; Altman, 1969; Gage, 2000). Comprehending the mechanisms that make lifelong neurogenesis possible has a clear interest for the better understanding of the basic principles that govern cellular and molecular interactions in the nervous system, as well as a relevant clinical interest. The limited ability of the CNS to generate new neurons in order to replace those that have been lost is a formidable obstacle for recovery from neuronal damage caused by injury or neurodegenerative disease. The idea that a more profound insight might allow us to overcome this obstacle is obviously quite appealing.

The olfactory system (OS) is an ideal system to study the process of neurogenesis, as it is known for its lifelong capacity to replenish cells lost during the natural turnover process, as well as its remarkable ability to regenerate after severe lesion. This system includes the olfactory bulb (OB) in the brain, the olfactory nerve (ON) and the olfactory epithelium (OE). The OE is part of the peripheral nervous system and connects to the OB via the ON. In addition to the already mentioned areas of the CNS, the OE also retains a stem cell population that guarantees neurogenesis throughout life (Moulton et al., 1970; Graziadei and Graziadei, 1978, 1979; Schwob, 2002; Huard et al., 1998). These stem cells continuously differentiate and give rise to new olfactory receptor neurons (ORNs), which are then reintegrated into an existing circuitry (Farbman, 1990; Roskams et al., 1996). For this to be possible, cell death must be highly regulated, and stem cells must pass through various stages of maturation before replacing cells as needed.

## 1.1. Basics of vertebrate olfaction

As mentioned above, the vertebrate OS includes the OE, found lining the interior nasal cavity; the ON, which is made up of bundled axons of ORNs that populate the OE and are responsible for odor detection; and the OB, the synaptic target of ORNs in the CNS, generally located in the most rostral part of the brain. The OE is made up of three main cell types (see **Fig. 1**) – supporting cells (SCs), that share both glial and epithelial cell properties; ORNs, that transmit olfactory information from the nose to the OB located in the brain; and a population of basal cells (BCs), proliferative cells which include the stem cells, as well as the various progenitor cells of the OE (Graziadei and Metcalf, 1971; Graziadei, 1971, 1973; Hansen et al., 1998; Murdoch and Roskams, 2007; Hassenklöver et al., 2009). Two morphologically distinct populations of basal cells have been identified in the murine OE - horizontal and globose BCs. The horizontal BCs have an elongated shape, are located atop the basal lamina, rarely divide, and therefore most likely represent the population of pluripotent stem cells of the OE (Beites et al., 2005; Murdoch and Roskams, 2007). Globose BCs on the other hand have been shown to constitute the major proliferating population of the OE. These have a round shape, reside immediately above the horizontal BCs, and include multipotent progenitors that give rise to ORNs and SCs (Beites et al., 2005; Murdoch and Roskams, 2007).

ORNs in vertebrates are bipolar neurons with an axon projecting into the OB and a dendrite that ends in a dendritic knob. This knob carries non-motile cilia or microvilli, which are specialized structures serving olfactory perception. This perception is initiated when odor molecules bind to specialized olfactory receptor proteins that belong to the G protein-coupled receptor superfamily. Five distinct olfactory receptor gene families have been described to date. In adult mammals, each individual ORN expresses only one type of olfactory receptor (Nef et al., 1992; Strotmann et al., 1992; Ressler et al., 1993; Vassar et al., 1993; Chess et al., 1994; Malnic et al., 1999; Mombaerts, 2004, 2006; see also Menini, 2010, Ch. 7), and all ORNs expressing the same olfactory receptor form a class and project an unbranched axon to one or more glomeruli within the OB (Ressler et al., 1994; Vassar et al., 1994; Mombaerts, 1996, 2006; see also Menini, 2010, Ch. 5). This common target structure, the glomerulus, contains the ORN synapses with the subsequent projection/second-order neurons, mitral and tufted cells. Odor-evoked activity patterns are processed by

the network of interneurons and are conveyed to multiple higher brain areas. These features represent the morphological basis of chemosensory brain maps connecting receptor specificities to the neuronal network of the OB.

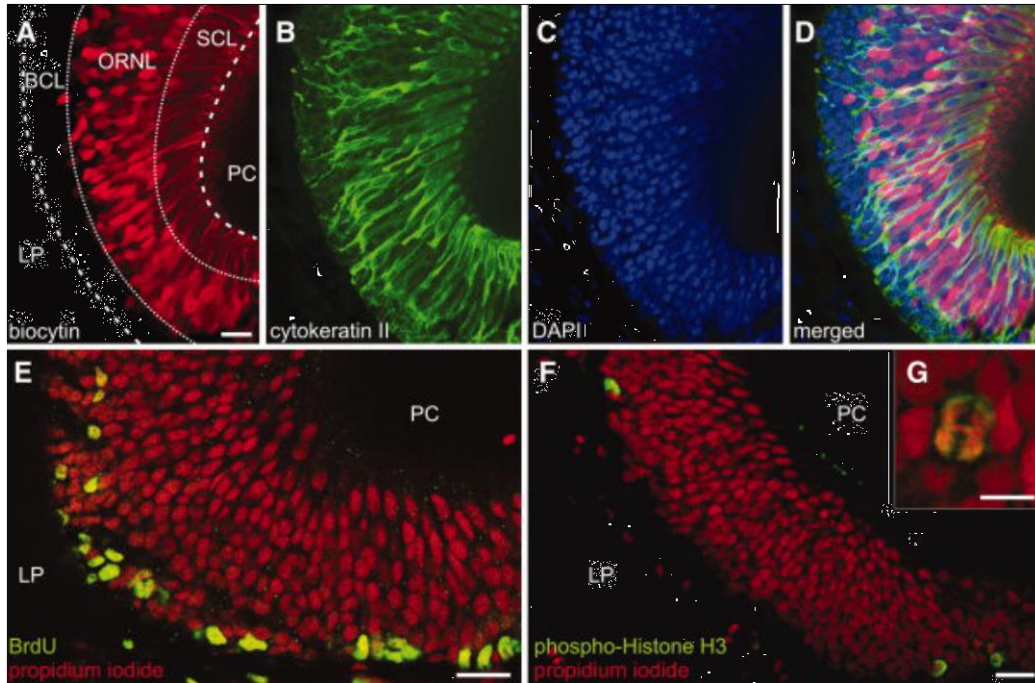


**Figure 1** - Location of the stem cell niche within the olfactory epithelium of larval *Xenopus laevis*. A. Slice of the olfactory epithelium (OE) with biocytin-streptavidin stained olfactory receptor neurons (ORNs). B. Supporting cell (SC) staining with an antibody against cytokeratin type II of the same slice. C. DAPI staining of all cell nuclei of the same slice. D. Overlay of ORNs (A, red fluorescence), SCs (B, green fluorescence), and all cell nuclei (C, blue fluorescence). Basal cells are biocytin-streptavidin- and cytokeratin II-negative and are located in the basal cell layer. The vast majority of BrdU-positive cells (E), and phospho-histone H3-positive cells (F) are confined to the basal cell layer of the OE. G. Higher magnification of a phospho-histone H3-positive basal cell in the late metaphase or the early anaphase of the mitotic cycle. Scale bars = 20  $\mu\text{m}$  (A, E, F), 5  $\mu\text{m}$  (G). Abbreviations: BCL, basal cell layer; BrdU, bromo-2'-deoxyuridine; DAPI, 4,6-diamidino-2-phenylindole; LP, lamina propria; ORNL, olfactory receptor neuron layer; PC, principal cavity; SCL, supporting cell layer. Reproduced from: [Hassenklöver et al., 2009](#).

Teleost fish have a single sensory surface that composes the OS, whereas several spatially segregated subsystems with different functional and molecular characteristics make up the mammalian OS. Although the steps involved in the evolutionary transition are largely unknown, the amphibian OS seems to represent an evolutionary intermediate and has been found to be well-suited for investigating the molecular forces that drive olfactory regionalization. Tetrapods possess at least two morphologically distinct nasal olfactory systems, the main and the accessory OS. The accessory OS, or vomeronasal system, is found only in tetrapods, having first appeared in amphibians, and is mainly involved in pheromone detection. The ORNs of these two systems possess differences

in olfactory receptor gene expression and in the transduction mechanisms responsible for olfactory signal transduction. In terrestrial vertebrates, most ORNs possess the canonical cyclic adenosine monophosphate (cAMP) -mediated transduction pathway (see also Menini, 2010, Ch. 8), but some ORN subgroups have been found to function via an alternate transduction cascade (Breer et al., 2006; Ma, 2007; see also Menini, 2010, Ch. 9). cAMP-independent transduction mechanisms have been found to be more common in aquatic vertebrates (Ma and Michel, 1998; Delay and Dionne, 2002; Manzini et al., 2002b; Hansen et al., 2003; Manzini and Schild, 2003), which can also be seen in the aquatic anuran amphibian, *Xenopus laevis*.

## 1.2. Olfaction in larval *Xenopus laevis*

For this project, the focus will be on the OS of larval *Xenopus laevis* as it is an ideal model organism for studying the basic mechanisms that govern olfaction and neurogenesis. The fertilized eggs of *Xenopus* develop into free swimming larvae and then metamorphose into juvenile frogs. The sorted cellular composition and the peripheral location make the OE readily accessible and easily manageable. Two separate olfactory organs, the vomeronasal organ and principal cavity (PC), are already distinguishable at around stage 40 larval *X. laevis* (stage classification according to Niewkoop and Faber, 1994). Around stage 51-52, a middle cavity starts to form and strongly expands during metamorphosis, while the PC is reorganized. The PC, the middle cavity and the vomeronasal organ form the peripheral olfactory organ found in the adult animal (Föske, 1934; Altner, 1962; Burd, 1991; Reiss and Burd, 1997a, 1997b; Hansen et al., 1998; Petti et al., 1999; Higgs and Burd, 2001). Axons of ORNs that reside in the PC project to the main OB. The main OE together with the main OB form the main OS. Larval *X. laevis* has a main OS, as well as a functional accessory OS, made up of the accessory OE, located in the vomeronasal organ, and the accessory OB, the synaptic target of vomeronasal receptor neurons, situated lateroventrally in relation to the main OB (see **Fig. 2**).

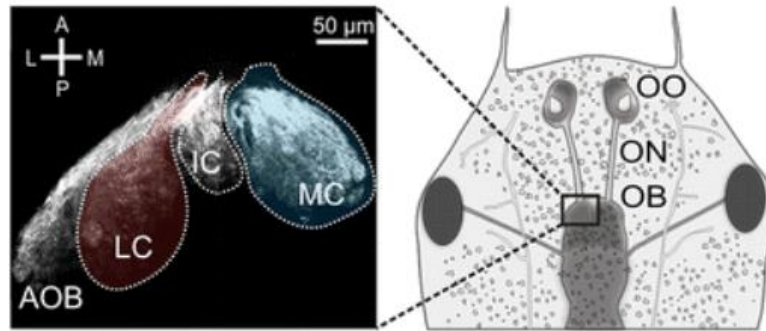


**Figure 2** - Olfactory system of larval *Xenopus laevis* highlighting the organization of the glomerular clusters in the olfactory bulb. The olfactory organ (OO) of *X. laevis* contains the olfactory epithelium. Olfactory sensory neurons that populate the olfactory epithelium project their axons into the olfactory bulb (OB) via the olfactory nerve (ON). The OB found in the anterior telencephalon in the brain contains glomerular structures, where synapses between sensory neurons and second order neurons occur. These glomeruli can be separated into spatially distinct clusters – lateral (LC), intermediate (IC), medial (MC) and small (not included in schematic). Apart from the main olfactory system larval *X. laevis* also possess a functional accessory olfactory system made up of the accessory olfactory epithelium found in the vomeronasal organ and the accessory olfactory bulb (AOB), the synaptic target of vomeronasal receptor neurons. To the left an image of one side of the olfactory bulb is visible, in which axons and glomeruli are stained. The dotted lines delineate the glomerular clusters visible in this image and the AOB, situated lateroventrally with respect to the main olfactory bulb. Abbreviations: AOB, accessory olfactory bulb; IC, intermediate cluster; LC, lateral cluster; MC, medial cluster; OB, olfactory bulb; ON, olfactory nerve; OO, olfactory organ. Adapted from: [Gliem et al., 2013](#).

As is the case in other amphibians, olfactory receptor genes of *X. laevis*, in certain aspects, represent an intermediate gene repertoire, having some similarities with terrestrial vertebrates and others with fish ([Niimura and Nei, 2005](#); [Saraiva and Korsching, 2007](#); [Shi and Zhang, 2007](#)). Olfactory receptors closely related to fish olfactory receptors, and those more closely related to mammals', have both been found to be expressed in the PC during larval stages ([Freitag et al., 1995](#); [Mezler et al., 1999](#)). After metamorphosis is complete, the PC is filled with air, and the middle cavity with water ([Altner, 1962](#); [Mezler et al., 1999](#)), whereas the vomeronasal organ is filled with water throughout the animal's life ([Altner, 1962](#)). Several findings suggest that some ORNs found in larval *X. laevis* express more than one type of olfactory receptor. For example, the number of different response profiles of individual ORNs to a variety of amino acids was found to be surprisingly high ([Manzini and Schild, 2004](#)). It was also shown that a narrowing of these response profiles takes place over ontogenetic stages, suggesting that the elevated number of response profiles could be related to the animals' ontogenetic stage. When compared, individual amino acid-sensitive glomeruli were found to be much more narrowly tuned than ORNs ([Manzini et al., 2007a](#)), and a narrowing of response profiles over ontogenetic stages was not observed ([Manzini et](#)



al., 2007a). Thus, it is possible that immature ORNs of *X. laevis*, that are still not fully connected to target glomeruli in the OB, express more than one amino-acid-sensitive olfactory receptor and lose all but one after having successfully reached their target glomerulus.

In premetamorphic stages of *X. laevis*, the glomerular layer of the main OB can be divided into a ventral part, with clearly discernable glomeruli, and a dorsal part, which consists of a fiber meshwork with some aggregations but no apparent structure (Fritz et al., 1996; Nezlin and Schild, 2000). In the glomerular layer of mammals, periglomerular glia cell bodies surround every glomerulus (Pinching and Powell, 1971; Chao et al., 1997), whereas in larval *X. laevis*, in similarity to what is seen in zebrafish, periglomerular cells do not form a wall around each individual glomerulus (Byrd and Brunjes, 1995; Nezlin and Schild, 2000; Nezlin et al., 2003). Around 350 glomeruli are found in the main OB of larval *X. laevis*, with diameters ranging between 10 and 40  $\mu\text{m}$  (Nezlin and Schild, 2000; Manzini et al., 2007b), which can be organized in at least 4 spatially distinct clusters – medial, intermediate, lateral, and small (Manzini et al., 2007b; see **Fig. 2**). The amount of mitral cells in the main OB of stage 54 larvae is not certain, but is in the range of 2000 (lower estimate - Nezlin and Schild, 2000) and 20,000 cells (upper estimate - Byrd and Burd, 1991). Axons of mitral cells of the main OB and accessory OB project to higher olfactory brain centers, forming the lateral olfactory tract.

Interestingly, a parallelization can be observed in the spatial propagation from olfactory sensory neurons to glomeruli, and from mitral cells to higher brain regions. Atypically, in larval *X. laevis*, ORN axons bifurcate various times before entering 2 or 3 glomeruli. The action potential resulting from these bifurcations could be important in introducing correlated signals to glomeruli during development in the OS (Nezlin and Schild, 2005). Also mitral cell dendrites bifurcate in a similar way, and mitral cells innervating the same glomerulus have been found to show synchrony (Chen et al., 2009). This may be important in odor recognition and for memory formation. The innervation of more than one glomerulus occurs in all ontogenetic stages of *Xenopus*, from larva to post-metamorphic frog. This atypical glomerular innervation pattern is not restricted to axons of immature ORNs, but is also found in mature neurons of the main and accessory OS (Hassenklöver and Manzini, 2013). So far, this wiring pattern has been found to be unique among all vertebrates investigated, and represents an olfactory

wiring strategy never before seen. These unique projection patterns could help increase the fidelity of transmission of a projection neuron to the dendrite, and/or alternately excite different receptor neurons. The slight temporal displacement of synaptic inputs could augment the synchronous activation of mitral cells within the target glomerulus. In higher vertebrates, this synchronous activation of mitral cells has been found to be related with glutamate spillover in glial-wrapped subcompartments of glomeruli (Schoppa and Westbrook, 2001). Contrary to what is seen in higher vertebrates (Chao et al., 1997; Kasowski et al., 1999), larval *X. laevis* glomeruli are not surrounded by glial processes and do not include glial-wrapped subcompartments (Nezlin et al., 2003). Nevertheless, this does not exclude the presence of a few periglomerular cells. Axonal splitting could therefore be an alternate way of guaranteeing synchrony of the mitral cells of individual glomeruli.

In the early diverging tetrapod *Xenopus laevis*, two odor-processing streams have been found to exist. These are well segregated in the main OB and only partially segregated in the OE of pre-metamorphic larvae. A laterally located odor-processing stream is made up of microvillus ORNs that respond to amino acids.  $G\alpha_o/G\alpha_i$  have been suggested as the most probable signal transducers involved in this odor-processing stream. A medial stream is also distinguishable, formed by ciliated ORNs that respond to aldehydes, alcohols, and ketones, with  $G\alpha_{olf}/cAMP$  as the most likely signal transducers. Some class II and class I olfactory receptors mimic the genetic spatial distribution observed in the medial stream, whereas a trace amine-associated receptor resembles the spatial pattern of the lateral odor-processing stream. Other olfactory receptors and odor responses are not lateralized, even in the OB, suggesting there is an incomplete segregation. Therefore, the OS of *X. laevis* seems to exhibit a state of segregation that is intermediate, and thus appears to be ideal for use in research on the molecular forces that drive olfactory regionalization. The vomeronasal organ of *X. laevis*, present already in the larval stages, is anatomically separated from the main OE. In similarity with the mammalian vomeronasal organ, vomeronasal receptor neurons of larval *X. laevis* express type II vomeronasal receptors. On the contrary, in contrast to mammals, type I vomeronasal receptors are expressed in the main OE (Gliem et al., 2013). This shows that olfactory receptor gene expression in *Xenopus* is also in a transitional state.

In more recent years, more focus has been put on the cellular interactions that take place in the OE. The impact of modulatory action in the OE on odorant transduction is becoming increasingly evident. Substances shown to be involved in signaling pathways in the OE and/or to influence peripheral odorant processing include neurotransmitters (Bouvet et al., 1988; Vargas and Lucero, 1999; Hegg and Lucero, 2004; Mousley et al., 2006), endocannabinoids (Czesnik et al., 2007), hormones (Arechiga and Alcocer, 1969; Kawai et al., 1999; Eisthen et al., 2000), and nucleotides (Hegg et al., 2003; Hassenklöver et al., 2008). ORN modulation by these substances ties odorant sensitivity to a variety of physiological processes, including local neuroprotection and regeneration. Studies have shown that cells found in the vertebrate OE express purinergic receptors (mouse: Hegg et al., 2003, 2008; larval *Xenopus laevis*: Czesnik et al., 2006; Hassenklöver et al., 2008). Application of adenosine triphosphate (ATP) to the OE of larval *X. laevis* leads to powerful increases in the intracellular calcium concentration ( $[Ca^{2+}]_i$ ) in SCs (Hassenklöver et al., 2008) that follow a characteristic spatial and temporal pattern. The initial  $[Ca^{2+}]_i$  increase always takes place in the most apical region of the SCs, and sequentially travels along their basal processes in the direction of the basal lamina, reliably suggesting that the purinergic receptors are located on the soma of SCs. The pharmacological characterization of purinergic responses indicates that extracellular nucleotides in the OE activate SCs via P2Y<sub>2</sub>/P2Y<sub>4</sub>-like receptors (Hassenklöver et al., 2008). Pharmacological studies done on the OE of larval *X. laevis* show that BCs express multiple P2Y receptors (Hassenklöver et al., 2009). Application of nucleotides to the main OE leads to strong wave-like  $[Ca^{2+}]_i$  increases in the SCs that propagate to the basal part of the main OE (Hassenklöver et al., 2008; Hegg et al., 2003). In other sensory systems, extracellular nucleotides have been shown to have neuromodulatory effects and to be involved in cellular signaling (Burnstock, 2007; Thorne and Housley, 1996). However, in contrast to what has been shown in mouse, larval *X. laevis* SCs, but not ORNs, respond to extracellular nucleotides (Hegg et al., 2003; Hassenklöver et al., 2008). Therefore the purinergic system in the OE of larval *X. laevis* seems to serve as an intraepithelial communication pathway from the most apical part of the OE to the basal lamina, via a nucleotide-induced “calcium wave”.

### 1.3. Regenerative capacity of the olfactory system

How do individual neurons go through the necessary stages of development and integrate functionally in a neuronal circuit? So far, knowledge on this topic has been derived predominantly from cell culture studies. Understanding how development of individual neurons occurs within an intact neuronal network *in vivo* is inherently difficult. During embryonic and early postnatal development most neurons are formed, and originate due to high neural stem cell activity. Once adulthood is reached, only two major neurogenic zones remain in the brain - the subventricular zone located in the lateral ventricles and the subgranular zone found in the dentate gyrus (Altman and Das, 1965; Altman, 1969; Gage, 2000). Neural stem cells pass through various phases of maturation, including proliferation, migration, differentiation, and integration, before becoming fully embedded in a neuronal circuit. While subventricular zone-derived cells migrate to the OB where they differentiate into at least two types of GABAergic neurons (Luskin, 1993; Lois and Alvarez-Buylla, 1994; Betarbet et al., 1996; Carleton et al., 2003), subgranular zone-derived cells are integrated into the dentate gyrus of the hippocampus (Cameron et al., 1993; Eriksson et al., 1998; Hastings and Gould, 1999; Seri et al., 2001; Kempermann et al., 2004; Seri et al., 2004; Halbach, 2007). If the adult mammalian brain is somehow lesioned, neurogenesis is upregulated particularly in the subventricular zone, which shows that the adult brain tries to repair itself. Newly formed neural precursors then migrate to the site of damage and generate neurons, but these generally are unable to integrate into the existing neuronal circuitry at the site of injury and therefore eventually die (Christie et al., 2013).

Evidence has shown that the level of neurogenesis in adult vertebrates is related to regenerative capacity post-injury (Doetsch and Scharff, 2001; Zupanc, 2001; Garcia-Verdugo et al., 2002). Fish and amphibians for example, have been shown to possess the most widespread ability for adult neurogenesis (Kirsche, 1967; Richter and Kranz, 1981; Chetverukhin and Polenov, 1993; Polenov and Chetverukhin, 1993; Bernocchi et al., 1990; Dawley et al., 2000; Raucci et al., 2006), and also the greatest ability to regenerate CNS injuries (Amphibians: Sibbing, 1953; Srebro, 1965; Filoni and Gibertini, 1969, 1971; Brockes and Kumar, 2002; Ferretti, 2004; Slack et al., 2004; Fish: Kirsche, 1950, 1960, 1965; Segaar, 1965; Richter, 1965, 1969; Zupanc, 2001). Comprehending the mechanisms that control endogenous proliferation and neurogenic permissiveness in the adult brain is extremely relevant to the development of

therapeutic approaches for treating brain damage, due to injury and disease. The widespread post-embryonic brain neurogenesis in non-mammalian vertebrates may be tied to brain growth due to growth of sensory systems (Evans, 1952; Brandstätter and Kotrschal, 1990; Marcus et al., 1999). Morphometric studies show that the cells in the brain of fish, amphibians and reptiles increase in number with age, body weight and length (Platel, 1974; López-García et al., 1984; Font et al., 2001; Martínez-Guijarro et al., 1994).

It has already been shown that *X. laevis* is able to regenerate after severe damage to the telencephalon, optic tectum and cerebellum, but only during larval stages (Srebro, 1964; Filoni and Gibertini, 1969, 1971; Filoni et al., 1995). Regeneration after damage is quite fast in juvenile frogs, being that the telencephalon regenerates already one month after lesion, and although morphological changes are still seen, correct connections are formed (Yoshino and Tochinai, 2004). Recently it has been shown that juvenile stage froglets can regenerate after severe telencephalic lesion both morphologically and functionally (Yoshino and Tochinai, 2006). Differences in the regenerative capacity of various brain regions of larval and metamorphosed *X. laevis* can be related to differences in the presence of undifferentiated cell populations (Filoni et al., 1995). During early-larval life, populations of proliferating cells are widespread in the brain, while in late-larval stages and after metamorphosis the cells are restricted to limited proliferation zones. This restriction occurs at later stages in the telencephalon and is related to the ability of the respective brain region to regenerate (Filoni et al., 1995). However, the main reason why post-metamorphic frogs are not able to regenerate severe telencephalic lesions seems to be due to a slow and imperfect sealing of the damaged area by ependymal cells (Yoshino and Tochinai, 2004).

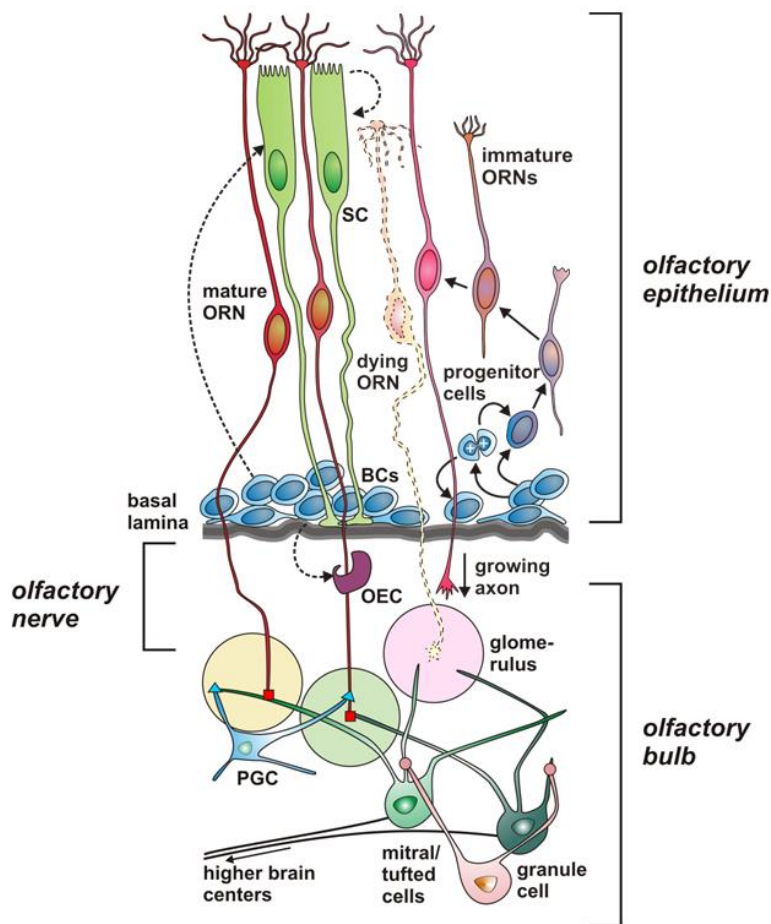


**Figure 3** - Schematic drawing of a section through the olfactory epithelium and the olfactory bulb in the normal olfactory system of larval *Xenopus laevis*. The three main cell types of the olfactory epithelium (OE) are olfactory receptor neurons (ORNs), non-neuronal supporting cells (SCs), and proliferative basal cells (BCs), the olfactory stem cells. Throughout life, the OE contains various immature ORNs, on their way to replace dying ORN. Basal cells may also give rise to SCs and olfactory ensheathing cells (OEC). Axons of ORNs penetrate the basal lamina of the OE, enter the olfactory bulb (OB), and terminate in olfactory glomeruli. There they form synapses with dendrites of mitral/ tufted cells, the second-order neurons of the olfactory system, and periglomerular cells (PGC). The axons of mitral/tufted cells merge together and convey the olfactory information to higher brain centers. The dendrites of granule cells, the most common type of interneurons of the OB, form modulatory synapses with dendrites of mitral/tufted cells. Abbreviations: BC, basal cell; PGC, periglomerular cell; SC, supporting cell; OEC, olfactory ensheathing cell; ORN, olfactory receptor neuron. Adapted from: [Manzini, 2015](#)

The first connections in the olfactory pathway are formed between the axon terminals of ORNs and the dendrites of mostly mitral/tufted cells, found in the glomeruli of the OB. These glutamatergic synapses are some of the most plastic in the CNS, with substantial changes that take place not only during developmental stages, but also during adulthood ([Mori and Sakano, 2011](#)). Not only does lifelong neurogenesis take place in the OE (see **Fig. 3**), but the OS has the ability to reconstitute after considerable damage, and the olfactory map recovers extensively ([Cheung et al., 2013](#)). In order to preserve the sense of smell, newly formed ORNs are reintegrated into the

olfactory circuit as needed (see **Fig. 3**). This is necessary because of the uniquely exposed and vulnerable location of ORNs in the OE. Neural stem cells found in the BC layer of the OE (near the basal lamina) maintain the lifelong production of new ORNs (Schwob, 2002). The OE possesses not only this capacity for normal turnover of ORNs, but also the ability to recover after substantial damage (Schwob, 2002). This shows that the OS can provide significant advantages for the study of the basic mechanisms that modulate stem cell renewal, neuronal regeneration, neuron development, synaptogenesis, and integration of newly formed neurons into an existing circuitry.

In *X. laevis*, during larval stages, the OS is already fully functional, and there is slow increase in the number of ORNs in the OE (Hansen et al., 1998; Byrd and Burd 2004). During this time in particular many axons grow in the direction of the OB, where they form synapses with glomeruli (Byrd and Burd, 2004). During metamorphosis the fully aquatic larvae transform into secondarily aquatic adult frogs, and during this process the OS is sequentially reorganized without losing its ability to process olfactory information (Dittrich et al., 2015). Most ORNs are replaced and substantial rewiring takes place (Dittrich et al., 2015). Although the OE has long been known as a site of long-term neurogenesis (e.g., Graziadei and Graziadei, 1979; Farbman, 1990; Carr and Farbman, 1992; Roskams et al., 1996; Calof et al., 1998; Huard et al., 1998; Schwob, 2002; Bauer et al., 2003), we still do not fully comprehend how the lifelong turnover of ORNs is regulated. Studies have shown that the proliferation and differentiation of OE progenitors is influenced by a balance of positive and negative regulatory factors released from various cells types (Bauer et al., 2003; Shou et al., 2000; Wu et al., 2003), a number of which have been identified, along with their receptors (reviewed in Murdoch and Roskams, 2007). Among proliferation-promoting factors are leukemia inhibitory factor (Bauer et al., 2003), basic fibroblast growth factors (DeHamer et al., 1994), epidermal growth factor, and transforming growth factor- $\alpha$  (Carter et al., 2004; Farbman and Buchholz, 1996). Growth and differentiation factor 11 and transforming growth factor- $\beta$  have been shown to act as proliferation-inhibiting factors (Wu et al., 2003). The effect of bone morphogenetic proteins has been shown to be dependent on their concentration, inhibiting neurogenesis in the OE at high concentrations and stimulating neurogenesis at low concentrations (Shou et al., 1999; Shou et al., 2000). Other substances such as neurotrophins (Simpson et al., 2003), pituitary adenylate cyclase-

activating polypeptide (Hegg et al., 2003), dopamine (Féron et al., 1999), nitric oxide (Sulz et al., 2006), insulin-like growth factor 1 (McCurdy et al., 2005), brain-derived neurotrophic factor, glial cell line-derived neurotrophic factor, and ciliary neurotrophic factor (Buckland and Cunningham, 1998) have also been suggested to have influence on the differentiation of OE progenitors. Evidence was more recently found that BCs, the OE stem cells, express purinergic receptors and that these receptors are involved in the regulation of the natural turnover of epithelial cells (Hassenklöver et al., 2009). Purinergic receptor subtypes expressed by BCs were identified and characterized, and studies revealed that blocking these receptors with a purinergic receptor antagonist reduced the proliferation rate of BCs. This finding strongly indicates that purinergic signaling may have an important role in the regulation of the natural cell turnover in the OE, and quite possibly the process of massive post-lesion reconstitution.

The peripheral location and the organized cellular composition make the OE of *X. laevis* easily accessible and manageable. Particularly throughout the larval period, the OS is ideal for in vivo microscopy due to elevated tissue transparency. Another relevant advantage is that in larval *X. laevis* ORNs can be activated by odorants, their natural stimuli. Therefore, the successful reconnection of new ORNs into the olfactory circuit can be easily tested by measuring odorant responses of individual ORNs, axons or glomeruli in the OB.



## 2. AIM OF THE MASTER THESIS

The *Xenopus laevis* OS, and in particular the larval system, is an important model for the study of the molecular and physiological mechanisms that control neuronal regeneration. This is because the mechanisms involved in cellular proliferation and differentiation are highly active. Also, the peripheral and exposed position, and the elevated tissue transparency facilitate the introduction of lesions in the OE, the ON and/or the OB (see **Fig. 4 (iv)**).

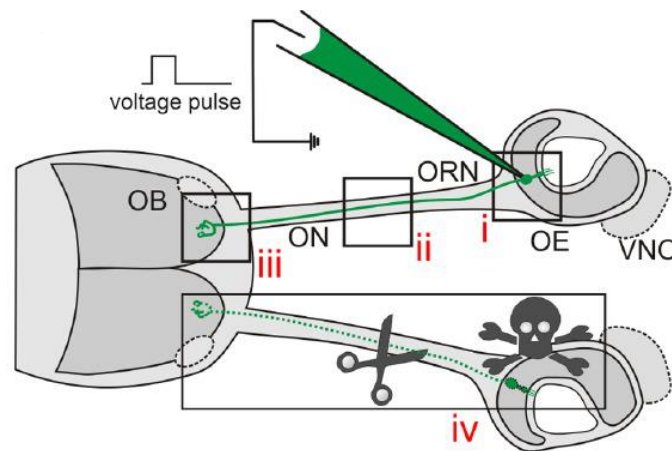


**Figure 4** - Schematic representation of the experimental approach used to study the process of regeneration in the olfactory system of *Xenopus laevis*. Olfactory receptor neurons (ORNs) in the olfactory epithelium (OE) of larval *Xenopus* can be labeled via spatially restricted electroporation of e.g., fluorescent dyes. Stained cells can be visualized in the OE (i), their axons can be followed through the olfactory nerve (ON, ii), and their axon terminals identified in the olfactory bulb (OB) (iii). ON transection induces cell death of the whole population of ORNs (iv). After ON transection newly formed ORNs can be monitored at different levels of the olfactory system (i, ii and iii). The vomeronasal organ (VNO) and the accessory OB are outlined by dotted lines. Abbreviations: OB, olfactory bulb; OE, olfactory epithelium; ON, olfactory nerve; ORN, olfactory receptor neuron; VNO, vomeronasal organ. Adapted from [Manzini, 2015](#)

For this thesis project, the process of regeneration after transection of the ON was studied. This method of injury was chosen as it was hypothesized that this would be a good method to target only ORNs without extensively disturbing other cell populations that may be involved in the process of regeneration. The aim of this thesis was to study the various events that occur during the process of regeneration of the OS after ON transection. Severing the connection between the OE and the OB leads to cell death and subsequently will allow us to observe neural stem/progenitor cell proliferation in the OE (see **Fig. 4 (i)**), axon development in the ON (see **Fig. 4 (ii)**), and the

reestablishment of synapses in glomeruli of the OB (see **Fig. 4 (iii)**). Combining electroporation of dextran-coupled dyes with the introduction of calcium sensitive dyes into ORNs and mitral/tufted cells allows acquisition of morphological and functional information. It is therefore possible to observe events related to stem/progenitor cell proliferation in the OE, axonal pathfinding and wiring, and finally to the formation of functional connections in the OB.

Sensory neuron labelling techniques were used to observe morphological changes in the ORN population; immunohistochemistry essays, to observe apoptotic events, cell proliferation in the BC layer, and SC structure in the OE; and functional calcium imaging techniques, to study changes in activity and evaluate loss of function and recovery in both the OE and OB. In this way, a reliable timeline for full recovery of function of the OS of larval *Xenopus laevis* was established, after ON transection.

## 3. MATERIAL AND METHODS

### 3.1. Animal selection and determination of ontogenetic stages

All *Xenopus laevis* larvae used in this study were raised in our breeding colony at the University of Göttingen. They were kept in water tanks (50 liters) at a water temperature of 19–22°C, and fed with algae (Dose Aquaristik, Bonn, Germany). The animals were staged according to Nieuwkoop and Faber (1994). All procedures for animal handling and tissue dissections were carried out according to the guidelines of the Göttingen University Committee for Ethics in Animal Experimentation.

### 3.2. Labeling of sensory neurons by olfactory nerve tracing and immunohistochemistry essays

Larval *Xenopus laevis* (larval stages 48–51) were anesthetized in 0.02% MS-222 (ethyl 3-aminobenzoate methanesulfonate; Sigma, Seelze, Germany), and unilateral olfactory nerve transection was performed with fine scissors. Biocytin (biotinyl-L-lysine, Life Technologies, Darmstadt, Germany) crystals were placed into the lesioned nerve, and the wound was closed with tissue adhesive (Histoacryl L; Braun, Tuttingen, Germany). Biocytin is a classical neuroanatomical tracer, commonly used to map brain connectivity. It is efficiently taken up by neurons and transported in both antero and retrograde directions. To visualize the neurons Alexa Fluor 568 Streptavidin was used, which is a Biotin binding protein covalently attached to a fluorescent marker. At different time points after Biocytin backfill animals were killed, and a block of tissue containing the olfactory organ, the olfactory nerve, and the anterior telencephalon was cut out. For bromodeoxyuridine (BrdU) immunostaining animals were kept 24 hours in beakers, containing 400 mL tap water and 12 mg (97.688 µM) 5-bromo-2'-deoxyuridine (B5002, Sigma; ≥99% (HPLC)) before being killed. The tissue blocks were fixed in 4% formaldehyde, washed in phosphate buffered saline (PBS), embedded in 5% low-melting-point agarose (Sigma) and cut horizontally into 75 µm slices with a vibratome

(VT 1200S; Leica, Bensheim, Germany). Slices were then washed in PBS containing 0.2% Triton X-100 (PBST), and used in 1 of 3 different immunohistochemistry essays.

Biocytin backfill coupled with Caspase-3 immunostaining: Alexa 568-conjugated streptavidin (Life Technologies) was applied at a final concentration of 5  $\mu\text{g/ml}$  in PBST, and slices were incubated at room-temperature for 1 hour, so as to visualize the biocytin-back-filled sensory neurons in the olfactory organ. Slices were repeatedly washed in PBS and nonspecific binding was blocked with 2% normal goat serum (NGS; ICN, Aurora, OH) in PBST for 1 hour, before incubation in primary antibody polyclonal anti-active caspase-3 (ab13847, derived from rabbit using a synthetic peptide corresponding to human active procaspase 3 aa 150–250 conjugated to keyhole limpet hemocyanin (KLH), RRID:AB\_443014; Abcam, Cambridge, United Kingdom; characterized by [Thompson and Brenowitz \(2010\)](#) and previously used in *Xenopus laevis* tissue by [Tseng et al., \(2007\)](#) and [Faulkner et al. \(2015\)](#)), diluted 1:600 in 2% NGS/PBST. This allows visualization of apoptotic cells (somata and axons). Primary antibodies were washed off with PBS, and Alexa 488-conjugated goat anti-rabbit secondary antibodies (Life Technologies) were applied at a dilution of 1:250 in 1% NGS/PBS for 1 hour.

Biocytin backfill coupled with BrdU immunostaining: Slices of BrdU treated animals were incubated in 1N HCl at 37°C for 45 minutes to denature DNA. Nonspecific binding was blocked with 2% NGS in PBST for 1 hour, before overnight incubation at 4°C with primary antibodies anti BrdU (monoclonal B2531, derived from mouse, Sigma), diluted 1:100 in 2% NGS/PBST. Primary antibodies were washed off with PBS, and Alexa 488-conjugated goat anti-mouse secondary antibodies (Life Technologies) were applied at a dilution of 1:250 in 1% NGS/PBS for 1 hour. This will allow visualization of cells in S phase present in the olfactory epithelium (OE). Secondary antibodies were washed off with PBS, and Alexa 568-conjugated streptavidin (Life Technologies) was applied at a final concentration of 5  $\mu\text{g/ml}$  in PBST, and slices were incubated at room-temperature for 1 hour, so as to visualize the biocytin-back-filled sensory neurons in the olfactory organ.

Biocytin backfill coupled with Cytokeratin immunostaining: Nonspecific binding was blocked with 2% NGS in PBST for 1 hour, before overnight incubation at 4°C with primary antibodies anti cytokeratin (1h5, monoclonal, derived from mouse),

diluted 1:1000 in 2% NGS/PBST. Primary antibodies were washed off with PBS, and Alexa 488-conjugated goat anti-mouse secondary antibodies (Life Technologies) were applied at a dilution of 1:250 in 1% NGS/PBS for 1 hour. This will allow visualization of cytokeratin type II containing filaments present in the OE (namely SCs). Secondary antibodies were washed off with PBS, and Alexa 568-conjugated streptavidin (Life Technologies) was applied at a final concentration of 5 µg/ml in PBST, and slices were incubated at room-temperature for 1 hour, so as to visualize the biocytin-back-filled sensory neurons in the olfactory organ.

Slices were then repeatedly rinsed in PBS, transferred to slides, and mounted in mounting medium (Dako, Hamburg, Germany) and image stacks of the OE were acquired with a laser scanning confocal microscope (LSM 510/Axiovert 100M; Zeiss, Jena, Germany). Image stacks of olfactory organ sections (75 µm thickness) were acquired at 1-2 µm intervals between the different planes. Multiple sections of each olfactory organ were acquired. The brightness and contrast of the images were adjusted.

Immunohistochemistry essays were performed to visualize alterations in the epithelia of the olfactory organ of *Xenopus* at different time points after ON transection. Animals were sacrificed 1, 2 and 3 days after unilateral transection and sensory neuron labelling (see above), as well as 1 week after transection (sensory neuron labeling in this case was performed on transected side 1 hour before dissection).

### **3.3. Calcium imaging in the olfactory epithelium**

Tissue slices were incubated with 125 µl of bath solution containing 50 µM Fluo-4/AM (Molecular Probes, Leiden, The Netherlands) and 50 µM MK571 (Alexis Biochemicals, Grünberg, Germany). Fluo-4/AM was dissolved in DMSO (Sigma, Deisenhofen, Germany) and Pluronic F-127 (Molecular Probes). The final concentrations of DMSO and Pluronic F-127 did not exceed 0.5% and 0.1%, respectively. To avoid multidrug resistance, transporter-mediated destaining of the slices, MK571, a specific inhibitor of the multidrug resistance-associated proteins, was added to the incubation solution (Manzini and Schild, 2003). After incubation at room temperature for 35 minutes, the dye solution was removed and replaced by bath solution. The slice was covered with a grid and placed on the stage of a confocal

microscope (LSM 780/Axio Examiner, Zeiss, Jena, Germany). Fluorescence images (excitation at 488 nm; emission > 495 nm) of the main OE were acquired at 1 Hz with 60 images per recording. The thickness of the optical slices excluded fluorescence detection from more than one cell layer.

The standard bath solution consisted of (in mM): 98 NaCl, 2 KCl, 1 CaCl<sub>2</sub>, 2 MgCl<sub>2</sub>, 5 glucose, 5 sodium-pyruvate, 10 HEPES with an osmolarity of 230 mOsmol/l and a pH of 7.8, which is the physiological pH in poikilothermic species (Howell et al., 1970). High K<sup>+</sup> bath solution consisted of (in mM): 17 NaCl, 80 KCl, 2 MgCl<sub>2</sub>, 1 CaCl<sub>2</sub>, 5 glucose, 5 sodium-pyruvate, 10 HEPES, 230 mOsmol/l, pH 7.8. The recording chamber was perfused with bath solution by gravity feed from a storage syringe through a funnel drug applicator (see Schild, 1985). The tip of the applicator was placed above the olfactory organ. The outflow of the bath solution was collected and discarded by a syringe needle which was also placed close to the olfactory organ. The advantage of this application system is that there is almost no mechanic stimulation of cells and an application of many nucleotides in succession is possible. Nucleotides were dissolved in bath solution and used at a final concentration of 100 μM in all conducted experiments. Nucleotide solutions were prepared immediately before the experiment and pipetted in the funnel without stopping the flow of the standard bath solution.

Image analysis was performed using custom programs written in MATLAB (MathWorks, Natick, USA). To facilitate selection of regions of interest, a “pixel correlation map” was obtained (see Junek et al., 2009). The fluorescence changes for individual cells are given as  $\Delta F/F = (F1-F2)/F2$ , where F1 was the fluorescent averaged over the pixels of a cell, while F2 was the average fluorescence of the same pixels before stimulus application averaged over 10 images.

### **3.4. Survey of olfactory sensory neuron re-innervation and olfactory bulb morphology**

Fluorophore-coupled dextran (Alexa 594 10 kD dextran; Life Technologies) was introduced into sensory neurons of the olfactory organ via electroporation (for details see Haas et al., 2002; Hassenklöver and Manzini, 2014). At the beginning of the experiment, larval albino *Xenopus* (stages 48–54), on which ON transection was

previously performed, were anesthetized in 0.02% MS-222, and Alexa 594 dextran crystals were introduced into both nasal cavities and dissolved in the residual moisture. Two thin, platinum electrodes were carefully placed in the nasal cavities. The electrodes were connected to a voltage pulse generator (ELP-01D; npi Electronics, Tamm, Germany), and 12 pulses (20–25 V, 25 msec duration at 2 Hz) with alternating polarity were applied. After the electroporation, animals were transferred into a beaker filled with fresh water for recovery. After ~5 minutes, the larvae woke from anesthesia and started normal swimming movements.

At different time points after transection, the tadpoles were sacrificed and the OB and ON were investigated via two-photon microscopy. Whole-mount preparations (including the anterior telencephalon, ON and olfactory organ) were placed in an imaging chamber, and an image stack of the whole intact OB was acquired from the ventral side (for details see [Hassenklöver and Manzini, 2014](#)). The brightness and contrast of image stacks were adjusted in the image processing software Fiji (<http://fiji.sc/Fiji>).

### **3.5. Calcium imaging in the olfactory bulb**

The following techniques were developed and performed by Thomas Offner, colleague and PhD student from the Manzini group - <http://olfsys.uni-goettingen.de/team.php>.

#### **3.5.1. Whole olfactory system preparation**

Tadpoles were chilled in iced water and killed by transection of the spinal cord. A rectangular tissue block containing the intact olfactory epithelia, olfactory nerves and the anterior part of the brain was extracted. After removal of ventral palatal connective tissue, the OB as well as the caudal part of the ON was ventrally exposed. To assure access of odorants to the main OE, excess tissue anterior to the nostril was removed using fine scissors.

### 3.5.2. Multiple cell bulk loading

The calcium indicator mix was prepared by dissolving 50 µg Fluo-4 AM (life technologies) in 5 µl DMSO (Sigma Aldrich) and adding 10 µl of Pluronic F-127 (0.2 µm filtered 10% (w/v), life technologies) as well as 35 µl of bath solution to a final volume of 50 µl. After a step of centrifugation to get rid of excess AM dye precipitate (1 minute, room temperature, 16.1 rcf), the supernatant was carefully removed. To prevent extrusion of the calcium indicator by the mitral/tufted cells through active transport, 3 µl of MK571 (10 mM; Enzo life sciences) were added to the mix (Manzini and Schild, 2003). Another 0.3 µl of 3 mM cascade blue dextran solution (life technologies) were added to visualize the mix distribution upon loading in the tissue under fluorescent illumination. Borosilicate glass pipettes of 10 to 15 MΩ resistances were pulled and filled with the calcium indicator mix. Whole mount preparations of the olfactory system were mechanically fixed using a metal grid with strings in a recording chamber containing bath solution. The pipette tip was carefully penetrated into the bulb with a micromanipulator in close proximity to the lateral cluster. Pressure was generated by compressing a cylinder filled with air. By opening a valve the pressure pulse was transferred via a tube system to the pipette to inject the dye into the tissue. The procedure was repeated up to three times at slightly different loci under observation via epifluorescent illumination until the region of interest was properly stained. After 35 minutes of incubation at room temperature successful uptake of fluo-4 AM by the mitral/tufted cells was observable as dim green fluorescence of their somata.

### 3.5.3. Fast multiphoton calcium imaging in the olfactory bulb

Calcium responses of the mitral/tufted cell tufts were imaged using an upright multiphoton microscope (Nikon A1R-MP, Nikon). An eight channel perfusion system, controlled by Valve Commander VC83 units (ALA Scientific Instruments), was connected to the setup for odorant application into the recording chamber. The funnel of the perfusion system was positioned in front of the main OE of the whole olfactory system preparation. To create a constant flow of odorants, a syringe connected to a suction pump was positioned caudally to the preparation. Whole volumes of the OB were measured over time with acquisition rates of 30-40 planes per second at a z-resolution of 3-5 µm. Alexa-594 and fluo-4 were both excited at a wavelength of 800 nm and laser powers between 10-20% (MaiTaiDeepSee). The emitted photons of the



different dyes were separated by emission filters of 500-550 nm for fluo-4 and 601-657 nm for Alexa-594. The main OE was stimulated with basic and aromatic L-amino acids: L-arginine, L-histidine, L-lysine, L-phenylalanine and L-tryptophane, individually or as a mixture at concentrations of 100  $\mu$ M. After 20 seconds of baseline fluorescence recording of the scanned volume the odorant solution was applied for 5 seconds and switched back to Ringer perfusion immediately afterwards. For each odorant application the recording lasted 2 minutes to include the whole calcium transient and let the ORNs recover to avoid adaptation effects.

#### **3.5.4. Analysis of calcium imaging data and reactive volume generation**

Changes in fluorescence measured in regions of interest are given as  $\Delta F/F$  values. The values were calculated for each pixel according to the following equation:  $\Delta F/F = (F - F_0)/F_0$ .  $F_0$  represents an averaged fluorescence value derived from the time interval prior to the stimulus and  $F$  is the actual fluorescence value of one pixel at one time point. For each single amino acid application experiment, a stack of difference images was created. The difference images were calculated for each plane by averaging the fluorescence value of the interval prior to stimulation and subtract this value from the mean peak response of the odor induced fluorescence peak (2-3 points for mean peak calculation). The stack of difference images was converted into a stack of binary images by adaptive thresholding. The resulting binary areas of each plane were assigned to individual groups by comparing their overlap with binary areas of neighbouring z-planes. This was done for each amino acid application experiment leading to a set of volumes representing the mitral/tufted cell somata and tufted regions reactive to the respective amino acids. To extract the glomerular volumes mitral/tufted cell bodies were manually removed from the measurements. The region of interest groups were used for 3D reconstruction of reactive volumes. Workflow scripts and analysis tools were kindly provided and programmed in MATLAB (Mathworks, Natick, USA) by Thomas Hassenklöver.

## 4. RESULTS

### 4.1. Changes in the olfactory epithelium after olfactory nerve transection

Transection of the olfactory nerve (ON) severs the connection between the olfactory epithelium (OE) and the olfactory bulb (OB). The synaptic connections between olfactory receptor neurons (ORNs) and second order neurons are lost due to ORN cell death caused by ON transection. However, after the damage caused by this lesion model, the olfactory system (OS) of larval *X. laevis* recovers function. ORN cell labelling via biocytin backfill of the ON, coupled with a variety of immunohistochemistry essays, made possible the detailed observation of the morphological changes that occur in the OE after ON transection.

Larval *X. laevis* animals were selected for ON transection based on stage of development, always falling between stages 48 and 52. The animals were staged according to [Nieuwkoop and Faber \(1994\)](#). These stages were considered optimum for this study because animals were developed enough to allow easy manipulation while not yet having initiated the process of metamorphosis, therefore guaranteeing stability in the OS throughout. To visualize changes in the ORN population 1, 2 and 3 days after transection of the ON, animals were transected and biocytin backfill was performed on the transected side, upon transection. In the case of animals to be sacrificed after 1 week, biocytin backfill was performed on the transected side 1 hour before dissection, to visualize the ORN population present at 1 week after transection of the ON. The tissue blocks obtained were sliced as described above and used for active Caspase-3, BrdU and Cytokeratin immunostainings. Active Caspase-3 immunostainings allowed the visualization of apoptotic events in the OE, BrdU immunostainings allowed the visualization of proliferative activity in the OE, and Cytokeratin immunostainings allowed the visualization of the SC structure.

#### 4.1.1. Apoptotic events

Results obtained show that active Caspase-3 positive cells increase substantially 24 hours after transection and peak in the quantity of apoptotic cells at 48 hours (see **Fig. 5 a-c, f**). After 72 hours caspase-3 positive cells are again similar to the control situation (see **Fig. 5 d**). There were some instances in which the amount of caspase-3 positive cells after 72 hours remained increased, as compared to control, but in all cases it is apparent that a substantial reduction from the elevated amount visible at 48 hours after transection occurs. After 1 week the transected side and control side appear to be the same, in relation to quantity of apoptotic cells (see **Fig. 5 a, e**).

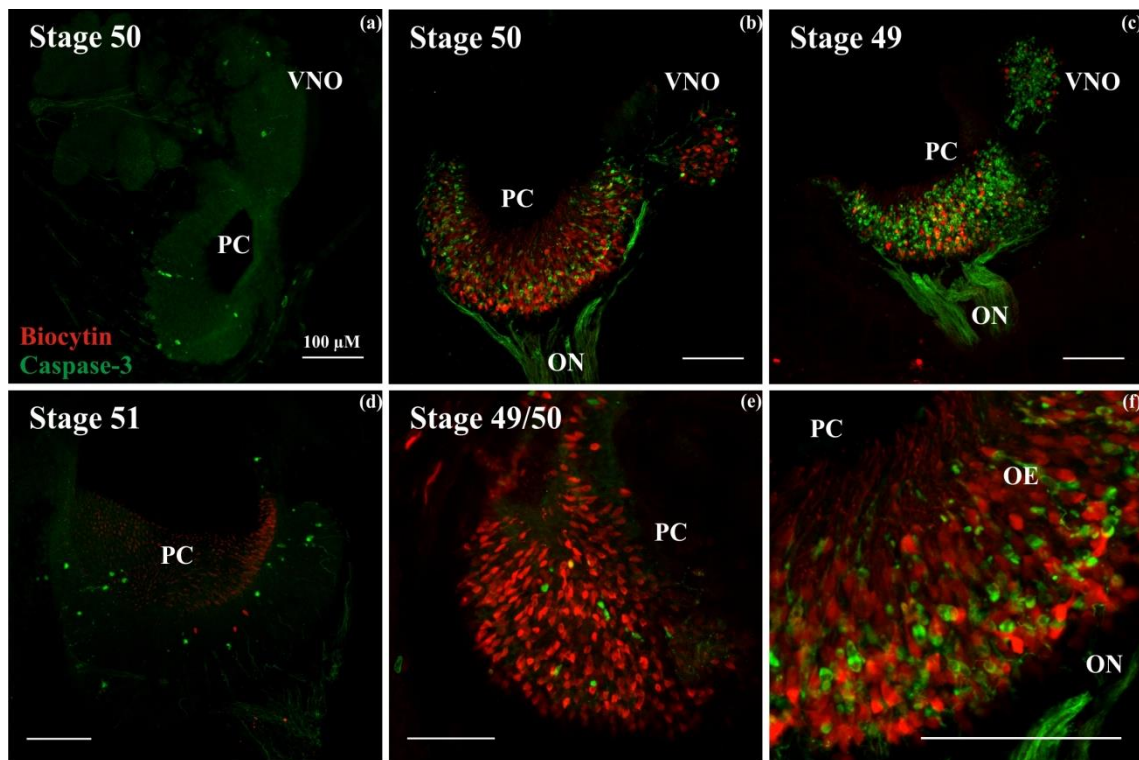


**Figure 5** – Changes in the olfactory epithelium: Biocytin backfill coupled to active caspase-3, at different time points after transection of the olfactory nerve. The olfactory epithelium of larval *Xenopus laevis* from stages 48-52 were used for biocytin backfill coupled to active caspase-3 staining, performed 1 to 3 days, and 1 week, after transection of the olfactory nerve. Biocytin backfill was performed on animals upon unilateral ON transection, with the exception of animals sacrificed after 1 week. In this case biocytin backfill was performed 1 hour before dissection. The olfactory organ on the non-transected side was used as control (a). Active caspase-3 positive cells (green) increase substantially 24 hours after transection (b) and peak at 48 hours (c). By day 3 (d), the OE looks similar to control situation, with just a slight increase in Caspase-3 positive cells. The majority of ORNs backfilled (red) upon transection disappear around 3 days after transection. 1 week after transection (e) the OE looks similar to the control situation with respect to Caspase-3 positive cells, and it also seems that it has been repopulated with ORNs. (f) Amplified section of the OE seen in (b). Abbreviations: OE, olfactory epithelium; ON, olfactory nerve; PC, principal cavity; VNO, vomeronasal organ.

#### 4.1.2. Proliferative activity

BrdU positive cells increase substantially in the BC layer and seem to maintain a higher number than control in the days following transection (see **Fig. 6 a-d, f**). After 1 week the control side and the transected side appear to be the same in relation to quantity of cells in S phase (see **Fig. 6 a, e**). However, further evaluation and cell quantification is necessary.

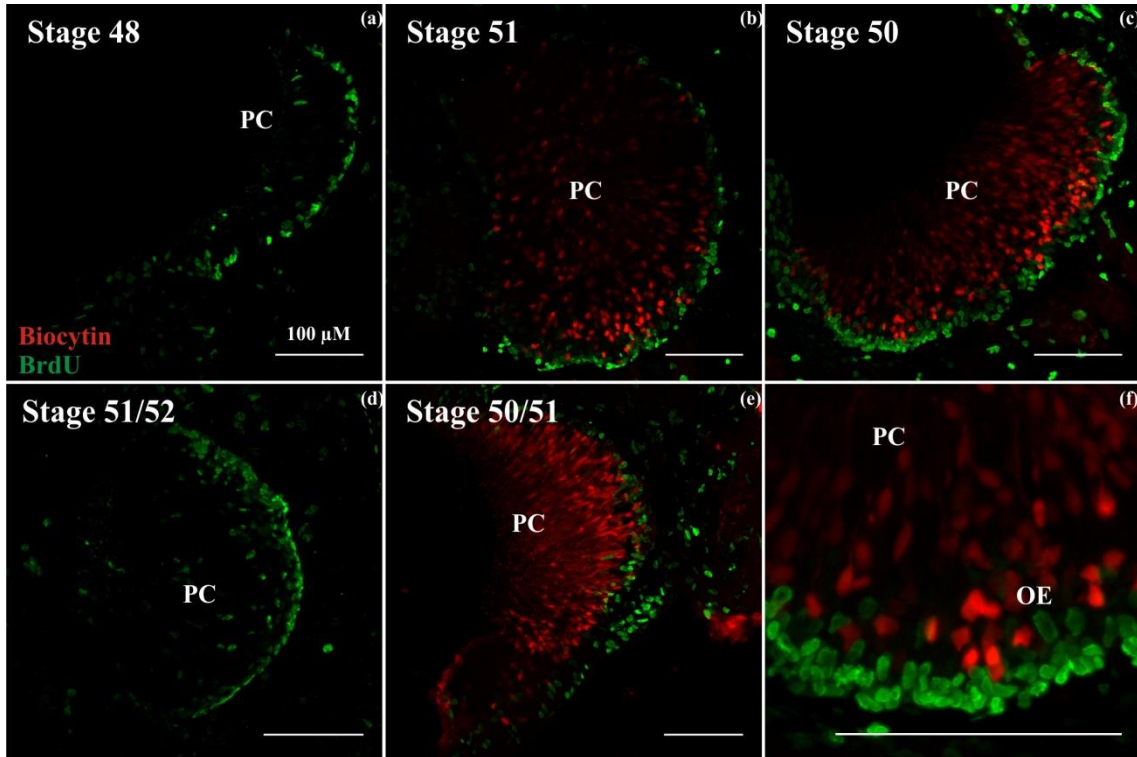


**Figure 6** - Changes in the olfactory epithelium: Biocytin backfill coupled to BrdU staining, at different time points after transection of the olfactory nerve. The olfactory epithelium of larval *Xenopus laevis* from stages 48-52 were used for biocytin backfill coupled to BrdU staining, performed 1 to 3 days, and 1 week, after transection of the olfactory nerve. Biocytin backfill was performed on animals upon unilateral ON transection, with the exception of animals sacrificed after 1 week. In this case biocytin backfill was performed 1 hour before dissection. The olfactory organ on the non-transected side was used as control (a). BrdU positive cells (green) found in the BCL increase substantially 24 hours after transection (b) and maintain higher numbers in the following days (c - 48 hours after transection, and d - 72 hours after transection). 1 week after transection (e) the OE looks similar to control situation with respect to BrdU positive cells, and it also seems that it has been repopulated with ORNs (red). (f) Amplified section of the OE seen in (c). Abbreviations: OE, olfactory epithelium; PC, principal cavity.

#### 4.1.3. Morphological integrity of supporting cells

Cytokeratin positive cells found in the SCL seem to maintain their integrity after ON transection and throughout recovery; with no obvious differences found at the different time points as compared to control (see **Fig. 7**).

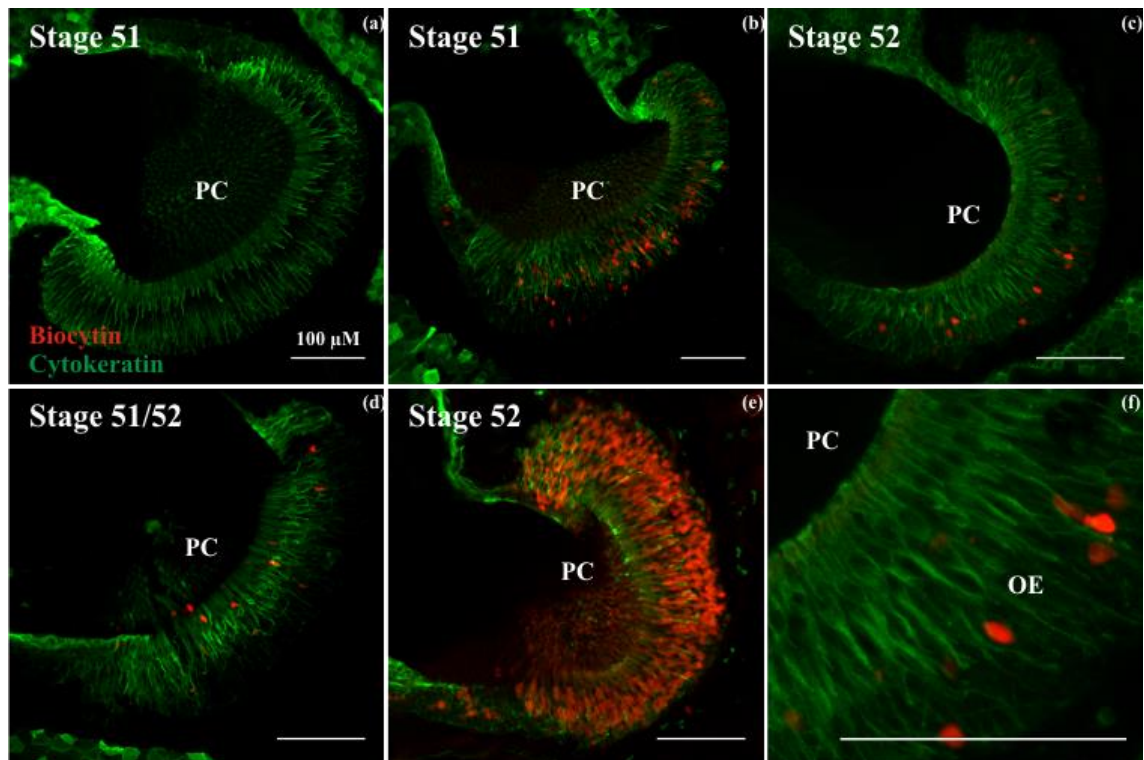


**Figure 7** – Changes in the olfactory epithelium: Biocytin backfill coupled to cyokeratin staining, at different time points after transection of the olfactory nerve. The olfactory epithelium of larval *Xenopus laevis* from stages 48-52 were used for biocytin backfill coupled to cyokeratin staining, performed 1 to 3 days, and 1 week, after transection of the olfactory nerve. Biocytin backfill was performed on animals upon unilateral ON transection, with the exception of animals sacrificed after 1 week. In this case biocytin backfill was performed 1 hour before dissection. The olfactory organ on the non-transected side was used as control (a). Cyokeratin filaments are found in SCs (green), therefore the use of specific markers allows visualization of SC morphology. SCs seem to maintain similar morphological structure throughout (b - 24 hours after transection, c - 48 hours after transection, and d - 72 hours after transection). 1 week after transection (e) the OE seems to have been repopulated with ORNs (red). (f) Amplified section of the OE seen in (c). Abbreviations: OE, olfactory epithelium; PC, principal cavity.

## 4.2. Calcium imaging in the olfactory epithelium

To find out how the functional integrity changes after ON transection, functional calcium imaging was performed on the OE of larval *X. laevis*, at different time points after transection of the ON.

ATP application to main OE preparations allowed confirmation that the BCL and the SCL seem to maintain not only morphological integrity but also functional integrity (see **Fig. 8**). After transection, cells found in the BC layer and SC layer still respond to ATP. Upon application of ATP,  $[Ca^{2+}]_i$  transients were visible in cells in the BC layer and SC layer. No  $[Ca^{2+}]_i$  transients were visible in cells of the ORN layer. The correlation maps show all responsive cells of the slice (**Fig. 8 (c)**). Specific transient

responses were mainly observable in SCs and BCs. These results were reproducible when ATP was applied several times. Virtually identical results were observed in all slices which were tested for their responsiveness to ATP.

It is possible to conclude from these results that supporting and basal cells are still able to detect and respond to nucleotides after ON transection. No conclusion about the number of responsive cells or changes of individual responses is possible. Additional experiments and further data analysis is necessary to conclude if any changes in the number of responsive cells occurs.

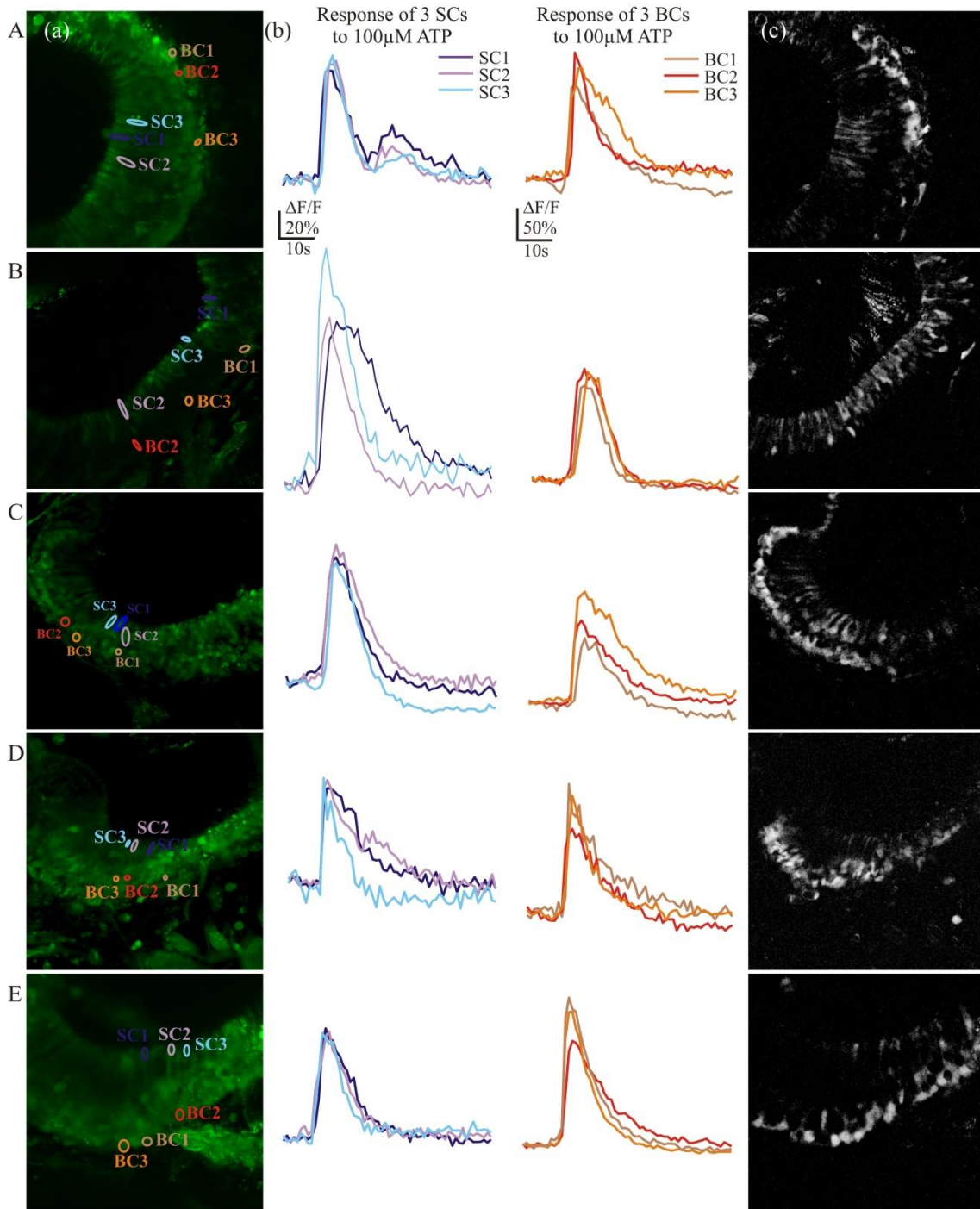


**Figure 8** - Functional integrity of supporting and basal cells after olfactory nerve transection. A. Calcium imaging performed on acute slices of the olfactory epithelium of a healthy animal, used as control. B. 24 hours after transection of the olfactory nerve. C. 48 hours after transection of the olfactory nerve. D. 72 hours after transection of the olfactory nerve. E. 1 week after transection of the olfactory nerve. (a) Image of an acute slice of the OE stained with  $\text{Ca}^{2+}$  indicator dye Fluo-4/AM. Application of 100  $\mu\text{M}$  of ATP induced  $[\text{Ca}^{2+}]_i$  transients in cells of the BC layer and SC layer. No apparent changes in  $\text{Ca}^{2+}$ -dependent fluorescence in cells of the ORN layer. (b) ATP-induced  $[\text{Ca}^{2+}]_i$  transients of individual cells randomly chosen from the SC layer (top, SC 1-3, blue traces) and BC layer (bottom, BC 1-3, orange traces). 100  $\mu\text{M}$  ATP was applied at the 10 second mark after initiating image acquisition. (c) A pixel correlation map of the same slice shows ATP-responsive cells bright against a dark background. Abbreviations: BC, basal cell; SC, supporting cell.

### 4.3. Changes in the olfactory bulb after olfactory nerve transection

#### 4.3.1. Morphological changes (axonal rewiring)

After unilateral ON transection sensory neuron labeling was performed via electroporation, and animals were sacrificed weekly, 1-7 weeks after the date of transection. Electroporation was performed 48 hours before the time of dissection for each time point. Whole mount preparation was performed and a stack of the OB and ON was acquired using 2-photon microscopy. This made the observation of morphological changes in the presynaptic side of the OB possible.

After 1 week, a small amount of ORNs seem to reach the very frontal portion of the OB (**Fig. 9 (b)**). After 2 weeks, substantial morphological changes are visible (**Fig. 9 (c)**). The OB is quite reduced in size but erratic projections of ORNs protrude into it, indicating that pioneering axons are actively searching for a post-synaptic partner.

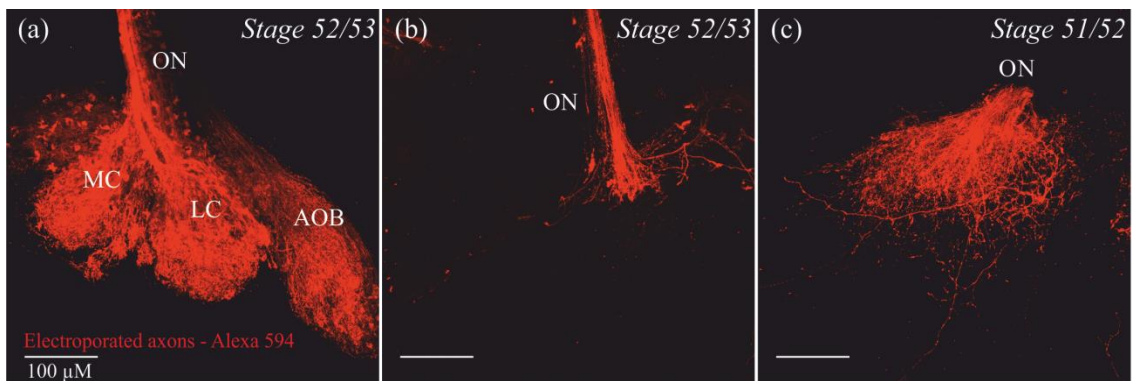


**Figure 9** - Reestablishment of olfactory bulb connectivity by sensory neuron axons after olfactory nerve transection. Electroporated ORNs in the OB and ON 1 and 2 weeks after transection of the ON. Fluorophore-coupled dextran was introduced into sensory neurons of the olfactory organ via electroporation (for details see [Haas et al., 2002](#); [Hassenklöver and Manzini, 2014](#)). Image stacks of the whole intact OB and ON were acquired via two-photon microscopy. (a) OB and ON of non-transected side used as control. Orientation of image is medial to lateral from left to right. The division of the OB in spatially distinct medial (MC) and lateral (LC) clusters is evident. (b) OB and ON on transected side, 1 week after transection. Orientation of image is lateral to medial from left to right. A small amount of axons reach the OB with no apparent innervation. The ON diameter is clearly reduced. (c) OB and ON 2 weeks after transection. Orientation of image is lateral to medial from left to right. Re-innervation is evidently taking place. Pioneering axons projecting into the OB are visible. Abbreviations: AOB, accessory olfactory bulb; LC, lateral cluster; MC, medial cluster; ON, olfactory nerve.

At 3 weeks, there seems to already be some morphological organization of the OB (**Fig. 10 (b)**). After 4 weeks, morphological structure of the OB is similar to control (**Fig. 10 (c)**). Although the OB on the transected side appears similar to control in



morphological organization, functional characterization of responses to stimulus is necessary to determine whether the OB is functional after the process of regeneration.

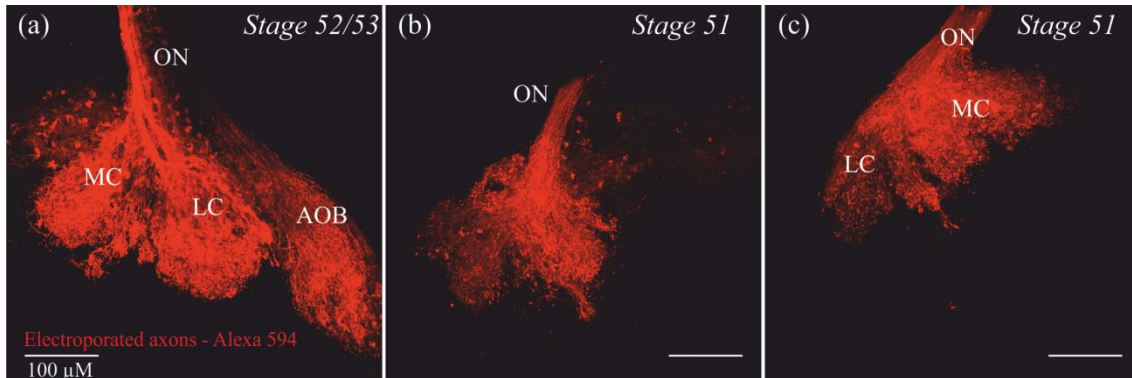


**Figure 10** - Successful reestablishment of olfactory bulb structure after olfactory nerve transection. Electroporated ORNs in the OB and ON 3 and 4 weeks after transection of the ON. Fluorophore-coupled dextran was introduced into sensory neurons of the olfactory organ via electroporation (for details see Haas et al., 2002; Hassenklöver and Manzini, 2014). Image stacks of the whole intact OB and ON were acquired via two-photon microscopy. (a) OB and ON of non-transected side used as control. Orientation of image is medial to lateral from left to right. The division of the OB in spatially distinct medial (MC) and lateral (LC) clusters is evident. (b) OB and ON 3 weeks after transection. Orientation of image is lateral to medial from left to right. Heightened axonal density is visible, as well as the beginning of spatial segregation of the OB in distinct clusters. (c) OB and ON 4 weeks after transection of the ON. Orientation of image is lateral to medial from left to right. Presynaptic division of axons projecting into distinct glomerular clusters is evident. Abbreviations: AOB, accessory olfactory bulb; LC, lateral cluster; MC, medial cluster; ON, olfactory nerve.

#### 4.3.2. Functional changes (cellular and glomerular responses)

Calcium imaging was performed on animals 3 days and 1-7 weeks after transection of the ON to evaluate at what time point responses to application of amino acids returns (**Fig. 11**). After 3 days no response was observed (**Fig. 11 (C)**), indication that the transection of the ON successfully severed the connection between the OE and the OB. Morphological analysis of the OB after 1 week allowed the observation of a small amount of ORNs reaching the very frontal portion of the OB. Calcium imaging at this time point resulted in only spontaneous response of mitral/tufted cells upon stimulus application, indicating that the proper function of glomeruli was disrupted by ON transection and has not regained function after 1 week. At 3 weeks, some slight responses are seen (**Fig. 11 (D)**). Distinct glomerular structures respond to the different amino acids applied (**Fig. 11 (F)**). After 7 weeks, responses in the OB are more widespread in the OB and are similar to control (**Fig 11 (E), (G)**).

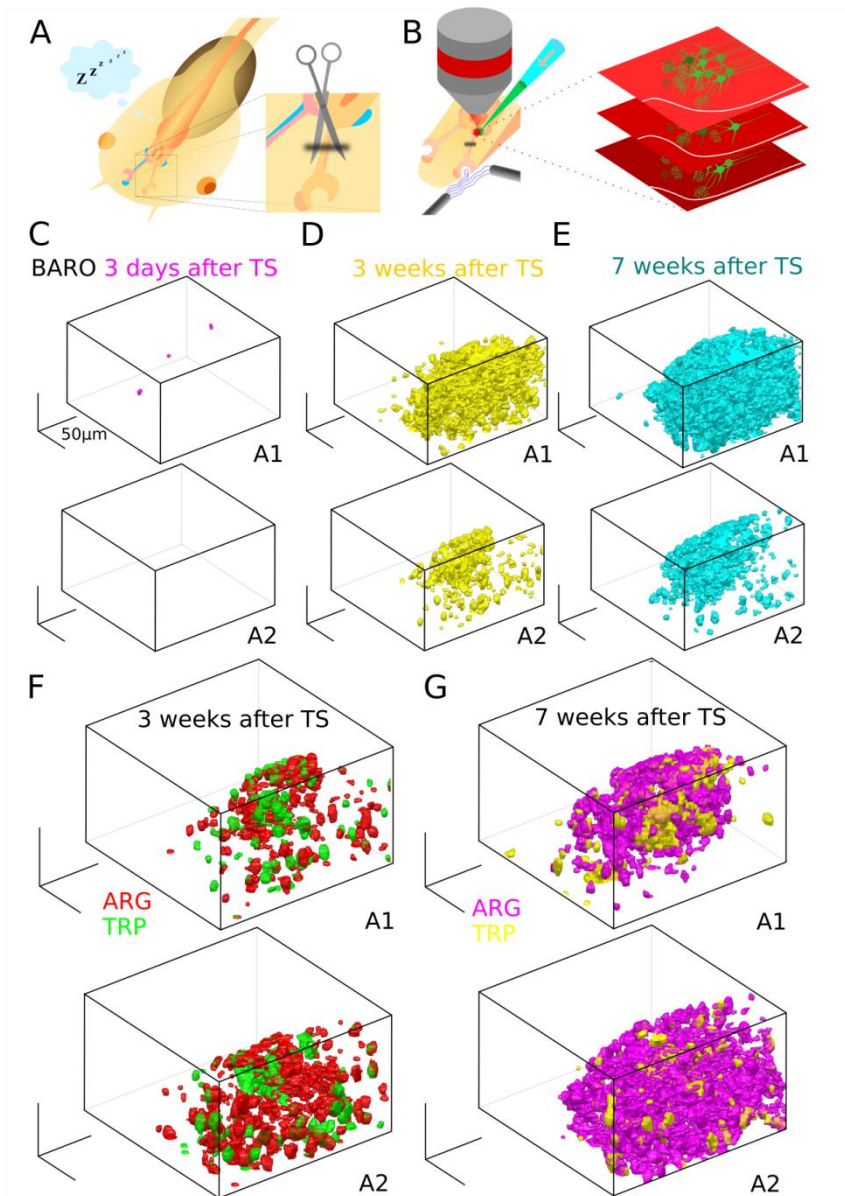


**Figure 11** - Loss and recovery of response in the olfactory bulb after olfactory nerve transection. A. Transection of the ON. B. Calcium indicator loading and multi-photon imaging of the OB. C. Responses of two different animals (A1 and A2) to application of basic-aromatic amino acid mixture, purple), 3 days after transection of the ON (TS). No responses are visible 3 days after transection of the ON, indicating that the synaptic connection between ORNs and the brain has been successfully severed and the OB has lost olfactory input. D. Responses of two different animals (A1 and A2) to application of BARO, 3 weeks after transection of the ON. In both animals responses to application of BARO (yellow) are visible, indicating that new synaptic connections have been established, 3 weeks after ON transection. E. Responses of two different animals (A1 and A2) to application of BARO, 7 weeks after transection of the ON. In both animals responses to application of BARO (cyan) are visible, and the density of responsive cells seems to have increased, when compared to 3 week animals (D). F. Responses of two different animals (A1 and A2) to application of 2 different single amino acids (ARG - arginine; TRP - tryptophane), 3 weeks after transection of the ON. In both animals responses to individually applied arginine (red) and tryptophane (green) is visible. The glomerular responses to the different amino acids are distinguishable. This indicates that new synaptic connections have been established and that different response profiles of glomeruli to amino acids is present. G. Responses of two different animals (A1 and A2) to application of arginine and tryptophane, 7 weeks after transection of the ON. In both animals responses to arginine (purple) and tryptophane (yellow) is visible and the density of responsive cells is increased, when compared to 3 week animals (F). Abbreviations: ARG, arginine; BARO, basic aromatic amino acid mix; TRP, tryptophan; TS, transection. Schematic created by Thomas Offner.

After 6-7 weeks responses seem to have fully recovered in all animals analysed. This indicates that the OS of larval *X. laevis* recovers morphologically and functionally 6-7 weeks after ON transection.

## 5. DISCUSSION

The aim of this thesis was to describe the morphological and functional alterations that occur over time in the olfactory system (OS) of larval *Xenopus laevis*, after transection of the olfactory nerve (ON). Transection of the ON leads to olfactory receptor neuron (ORN) cell death, and to the loss of synaptic connection between the olfactory epithelium (OE) and the olfactory bulb (OB) (see **Fig. 12**). This, in turn, leads to the loss of function of the OB. Results obtained using immunohistochemistry essays, as well as sensory neuron labeling and functional calcium imaging techniques, indicate that cell death reaches its peak 48 hours after transection, and that proliferating stem cells found in the basal cell layer of the OE are quickly upregulated after lesion. Supporting cells (SCs) seem to maintain both morphological and functional integrity after transection of the ON, indicating that the SC layer is not substantially damaged by this lesion. The OE recovers its original morphological structure 1 week after transection, at which time the first axons reach the olfactory bulb and begin the process of re-innervation (see **Fig. 13**). Spontaneous activity of mitral/tufted cells occurs in the olfactory bulb during the first weeks after transection but no odor-induced activity is observed. After 3-4 weeks glomerular responses were observed in some animals upon application of stimulus, but the response and glomerular morphology are clearly altered as compared to control. After 6-7 weeks responses seem to have fully recovered, indicating that the OS of larval *X. laevis* recovers morphologically and functionally 6-7 weeks after ON transection.

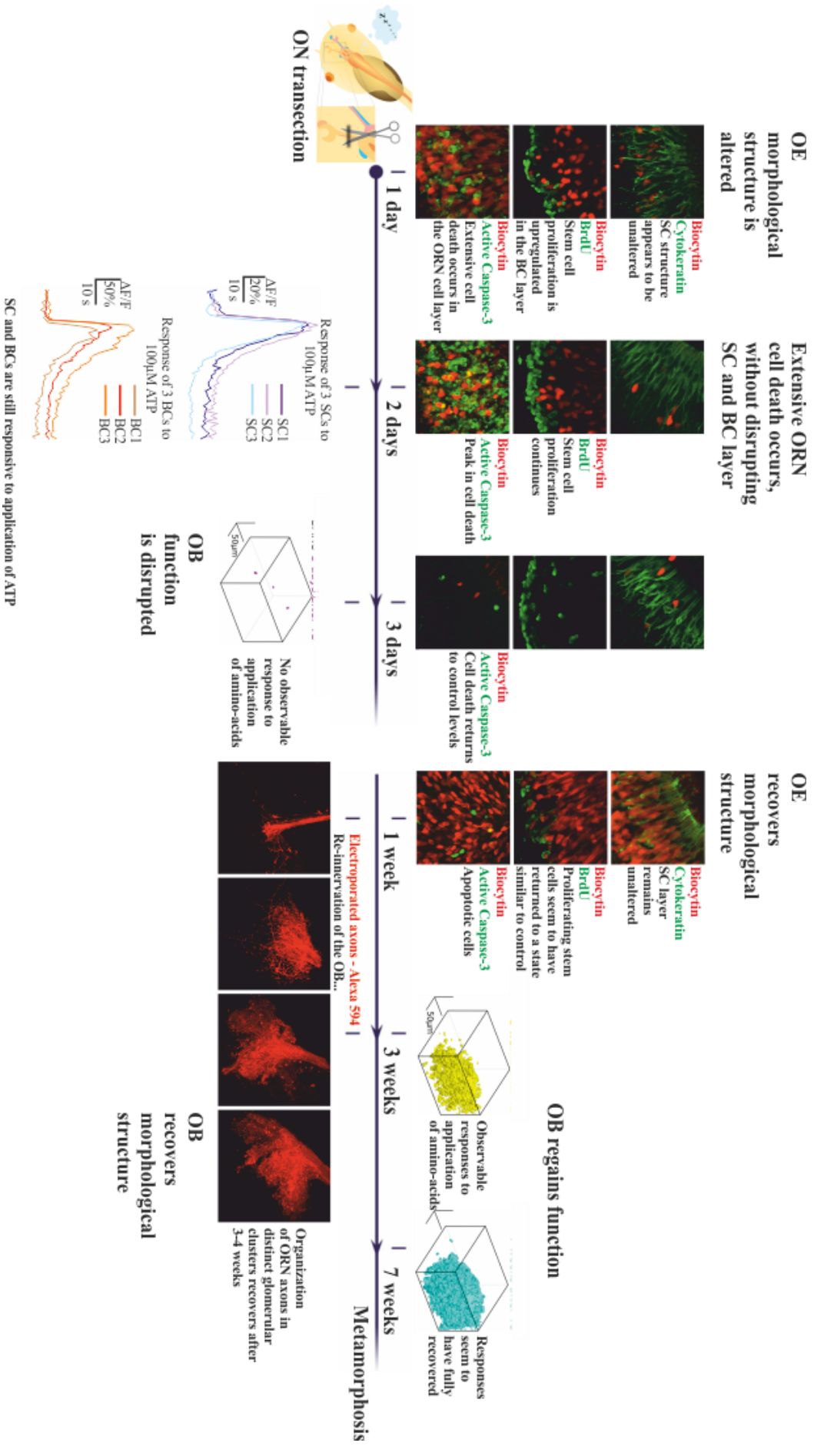


**Figure 12** - Olfactory system regains structural and functional integrity over the course of 7 weeks after transection of the olfactory nerve. Timeline begins with transection of the olfactory nerve (ON). 1 day after transection of the ON disruption of the olfactory epithelium (OE) occurs, mainly due to increased cell death in the olfactory receptor neuron layer. There is also an increase in proliferating cells in the basal cell layer. The supporting cell layer seems to remain unaltered in the days following ON transection. Loss of function in the olfactory bulb (OB) after ON transection was observed using functional calcium imaging techniques. The OB no longer responds to application of amino-acid mix. The OE recovers its original morphological structure 1 week after transection, at which time the first axons reach the olfactory bulb and begin the process of re-innervation. After 3-4 weeks the distinct glomerular clustering in the OB is again visible. Responses to amino-acids are again visible 3 weeks after transection of the OB and seem to fully recover in all animals observed 7 weeks after transection. Abbreviations: BC, basal cell; OB, olfactory bulb; OE, olfactory epithelium; ON, olfactory nerve; ORN, olfactory receptor neuron; SC, supporting cell.

### **5.1. Olfactory receptor neuron cell death and basal cell proliferation are tightly coupled and highly regulated**

After ON transection, controlled cell death in the ORN population is followed by stem cell proliferation in the BC layer in order to replace cells as needed. During the initial phase of apoptosis, the signal for cell death leads to the activation of an intracellular cascade of events that may include the production of Par-4, increased levels of oxyradicals and  $Ca^{2+}$ , and translocation of pro-apoptotic Bcl-2 family members (Bax and Bad) to the mitochondrial membrane (Yuan and Yankner, 2000; Cheung et al., 2005). During the effector phase of apoptosis increased mitochondrial  $Ca^{2+}$  and oxyradical levels occurs (Greenlund et al., 1995; Mattson, 2007), along with formation of permeability transition pores in the mitochondrial membrane (Brenner and Moulin, 2012), and release of cytochrome c into the cytoplasm (Cai et al., 1998; Liu et al., 1996), which forms a complex with apoptotic protease-activating factor 1 and caspase-9. Activated caspase-9, in turn, activates caspase-3, leading to the beginning of the degradation phase of apoptosis. During this phase, numerous caspase and other enzyme substrates are cleaved, leading to characteristic alterations in the plasma membrane (blebbing and exposure of phosphatidylserine on the cell surface, a signal that activates cell phagocytosis by macrophages/microglia) (Slee et al., 1999; Coleman et al., 2001). During the final phases, the nuclear chromatin condenses and becomes fragmented. As observed after ON transection in larval *X. laevis*, after the extensive cell death that follows ON transection, 72 hours later the majority of apoptotic cells have been cleared away from the OE, presumably due to phagocytosis by macrophages/microglia.

Many signals can initiate or 'trigger' apoptosis in neurons. The best-studied signal is lack of neurotrophic factor support, which may trigger apoptosis during development of the nervous system and possibly in neurodegenerative disorders (Oppenheim, 1991; Mattson et al., 1997; McKay et al., 1999). Most neurons in the mammalian CNS possess receptors for the excitatory neurotransmitter glutamate, whose overactivation can induce apoptosis by a mechanism involving calcium influx (Ankarcrona et al., 1995; Glazner et al., 2000). Oxidative stress can also trigger neuronal death, in which free radicals (such as the superoxide anion radical and the hydroxyl radical) damage cellular lipids, proteins and nucleic acids by attacking chemical bonds in those molecules (Sastry and Rao, 2000; Mattson et al., 1998). Environmental toxins can induce neuronal apoptosis, and several such toxins can induce specific patterns of brain damage (Beal, 1995; Duan et al., 1999). There are several prominent anti-apoptotic signalling pathways that contribute to neuronal survival (Mattson et al., 1997). Neurotrophic factors have been identified that can protect neurons against apoptosis by activating receptors linked through kinase cascades to production of cell-survival-promoting proteins. For example, brain-derived neurotrophic factor or (BDNF), nerve growth factor or (NGF) and basic fibroblast growth factor or (bFGF) can prevent death of cultured neurons, in part by stimulating production of antioxidant enzymes, Bcl-2 family members and proteins involved in regulation of calcium homeostasis (Mattson et al., 1997; Tamatani et al., 1998). Cytokines such as tumour necrosis factor- $\alpha$  (TNF- $\alpha$ ), ciliary neurotrophic factor (CNTF) and leukaemia inhibitory factor (LIF) can prevent neuronal death in experimental models of natural neuronal death and neurodegenerative disorders (Hagg et al., 1993; Middleton et al., 2000; Mattson et al., 2000).

ORN cell death and BC proliferation are tightly coupled events. Results obtained indicate that ORN death reaches its peak 2 days after transection and that proliferating stem cells found in the BCL of the OE are upregulated in the days immediately following lesion. These results are in line with previous studies showing that cell death and replacement of ORNs are tightly coupled (Costanzo and Graziadei, 1983; Schwob et al., 1992). In mouse, ORNs that are inhibited from environmental exposure and stimulation by naris occlusion demonstrate enhanced lifespan, and a reduction in ORN turnover and progenitor division. Reversal of occlusion stimulates progenitor activity and the ORN population is restored within 6-10 days (Cummings and Brunjes, 1997).

Surgical removal of the OB induces a retrograde wave of apoptosis in ORNs within 72 hours after bullectomy (Cowan et al., 2001), stimulating mitosis in local progenitor cell populations (Graziadei and Graziadei, 1979). ORNs are then generated from adult OE-residing progenitors by 2-3 weeks after removal of OB (Costanzo and Graziadei, 1983; Schwob et al., 1992). An intranasal chemical lesion applied directly to the nasal cavity leaves the OB available for axon re-targeting, but also destroys multiple cell types. Detergent (Triton X-100), zinc sulphate (ZnSO<sub>4</sub>) (Harding et al., 1978), methylbromide (MeBr) gas (Schwob et al., 1995) and the thyroid drug, methimazole (Bergman et al., 2002; Bergström et al., 2003) have all demonstrated efficacy in inducing widespread OE cell loss, and stimulating regeneration of multiple lineages. If the damage is too excessive, reconstitution can be incomplete, and respiratory epithelium will replace the OE (Schwob, 2002). After MeBr treatment, proliferation occurs 1-2 days following lesion, peaking after 1 week and continuing for up to 4 weeks. The OE is almost fully restored to its pre-lesion state by 6 weeks.

## **5.2. Olfactory nerve transection does not eliminate supporting and basal cell function**

ON transection leads to ORN cell death but does not lead to extensive damage in other cell populations in the OE. This was shown using functional calcium imaging experiments in the OE. SC and BCs in the OE have been shown to express purinergic receptors that respond to ATP. Upon ATP application to the OE at different time points after transection of the ON it was verified that the characteristic nucleotide-induced “calcium wave” still occurs in the OE after transection. Purinergic signaling has been linked to neuro-regenerative processes in the peripheral nervous system.

The amount of cells in S phase increases drastically in the BC layer in the days immediately following lesion. It was previously shown that the BC layer of the OE of larval *Xenopus* is composed of about 3-4 cell sublayers that include 2 main cell types - elongated BCs with long interlaced cytoplasmatic extensions, found adjacent to the basal lamina, and polyhedral BCs that reside immediately above the elongated BCs (Hansen et al., 1998; Hassenklöver et al., 2009). These two cell types could be equivalent to horizontal and globose BCs, present in the BC layer of mouse (Murdoch



and Roskams, 2007; Beites et al., 2005). In mouse, horizontal BCs, which have an elongated shape, are located above the basal lamina, seldomly divide, and are likely to represent the multipotent stem cells of the OE (Murdoch and Roskams, 2007; Beites et al., 2005). Studies have shown that the globose BCs are the major proliferating population in the OE, are found immediately above the horizontal BCs, are round-shaped, and contain multipotent progenitors that differentiate and give rise to ORNs and SCs (Murdoch and Roskams, 2007; Beites et al., 2005). In the normal situation in which the animal is healthy, the BC population is active to a degree that allows regulated maintenance of the OE, replacing cells lost during turnover. After lesion, the drastically increased number of proliferating cells in the BC layer indicates that a signaling mechanism must exist to activate this response to acute damage. Purinergic signaling has been proposed as a mode of intraepithelial signaling and induction of stem cell proliferation. This is supported by the fact that both SCs and BCs express purinergic receptors that respond to application of nucleotides by generating a characteristic  $\text{Ca}^{2+}$  wave that moves from the most apical part of the epithelium to the basal region (Hassenklöver et al., 2008, 2009). Nucleotides released as ORNs die could trigger intracellular  $\text{Ca}^{2+}$  increase in SCs, and subsequently transmit the information to the BCL. Since it has been shown that neuronal stem cells reside in this layer it is possible that ORN cell death provokes upregulation of BCs in this way. It was hypothesized that response to ATP could be higher in transected animals than in control animals, as purinergic signaling has been linked to neuroregenerative processes. Although this hypothesis was not excluded, additional experiments are required for significant conclusions to be made.

In studies using rodent OS as model for neurogenesis after lesion, it is clear that the ORN replacement program is not uniform across all turbinates (Weiler and Farbman, 1997; Cowan et al., 2001; Carter et al., 2004). Lesion-induced ORN neurogenesis seems to be controlled by both the demand for replacement (loss of ORNs) and the degree of availability and activity of local endogenous progenitors. During post-bulbectomy neurogenesis, rather than undergoing uniform neuronal replacement following death of mature ORNs (Moulton, 1974; Càmarà and Harding 1984; Carr and Farbman, 1992; Gordon et al., 1995; Huard et al., 1998; Schwob, 2002), adjacent regions of OE in a given turbinate demonstrate a highly patchy pattern of neurogenesis. This is likely due to (i) a dynamic spatiotemporal retrograde ORN

apoptosis leading to localized changes in feedback induction/repression signaling (Cowan et al., 2001; Bauer et al., 2003); (ii) a change in lateral inhibition from neighboring cells that relieve inhibitory mechanisms that normally allow only a subset of BCs to respond to a mitotic stimulus (Shou et al., 2000; Morrison, 2001; Watt, 2001) and (iii) stimulation of neurogenesis from underlying olfactory ensheathing cells that are no longer in contact with axons. In the contralateral OE, a delayed significant increase in local basal cell mitosis also suggests that a feedback loop could exist from the central nervous system that senses the loss of ipsilateral ORN input and instructs the contralateral OE to compensate (Carter et al., 2004). ORN genesis is thus clearly controlled by the balance of positive regulatory factors from cells (e.g. apoptotic ORNs, macrophages, olfactory ensheathing cells) that sense a need for more ORNs and stimulate mitosis and differentiation, and a reduction in negative feedback from mature ORNs to inhibit additional ORN production (Shou et al., 2000; Bauer et al., 2003; Wu et al., 2003). Factors that have been shown to positively regulate ORN genesis include LIF, FGF, EGF and TGF- $\alpha$ . Factors that have been shown to negatively regulate ORN genesis include the TGF- $\beta$  superfamily of growth factors, which includes TGF- $\beta$ , activins and BMPs. BMPs are morphogenetic proteins whose effects can vary according to their concentration and target cell (Mehler et al., 2000). Many of these factors play important roles during embryonic and post-natal nervous system formation. As they have also been found to be present during processes of massive recovery after lesion this suggests that there is a correlation between development and regeneration. These tissues may recapitulate some aspects of the developmental programs used in the initial creation of the injured tissues (Brookes, 1997; Brookes and Kumar, 2002).

In different lesion models, the time course and pattern of ORN replacement clearly depends both on the type and rate of ORN death, and the extent of cell types lost (Carter et al., 2004). It would be interesting to compare the differences observed in the regenerative process in larval *X. laevis*, under varied lesion models. In the model chosen for this study - transection of the ON - only the ORNs are targeted for cell death. In this way, the OB is intact and available for re-targeting by newly formed pioneering axons, and the proliferating stem cell population in the OE is left unharmed. It would be interesting to compare these results with lesion models in which various cell populations in the OE are damaged and/or the OB is made unavailable for ORN targeting.

### 5.3. Glomerular responses are lost after olfactory nerve transection, and recover after 6-7 weeks

After ON transection in larval *X. laevis* it appears that the OE recovers morphological structure 1 week after unilateral transection of the ON, at which time the first axons reach the olfactory bulb (OB) and begin the process of reinnervation. In the weeks following lesion, pioneering axons are visible and these apparently are successful in re-targeting the OB. Only spontaneous activity of mitral/tufted cells is observed in the OB during the first weeks after transection. This indicates that mitral/tufted cells persist in the OB after extensive ORN cell death. It could be that M/TCs in larval *X. laevis* survive after losing their pre-synaptic partner and continue to show spontaneous activity. This spontaneous activity could also be a modulatory mechanism during the process of axon retargeting, assisting in the correct reconnection of synaptic partners. After 3-4 weeks glomerular responses were observed in some animals upon odor stimulus application, but the response and glomerular morphology were clearly altered when compared to non-transected control side of OB.

How do the odor representations carried by ORN inputs to the OB recover after massive loss and regeneration of the ORN population? The OS of larval *X. laevis* seems to recover morphologically and functionally 6-7 weeks after unilateral transection of the ON. This recovery is apparently quite extensive and function is clearly restored, but it would be interesting to see what alterations occur after lesion, at a more detailed level. Once the spatiotemporal odor evoked map has been established for larval *X. laevis*, under normal conditions, a comparison with altered models subjected to different forms of lesion will be possible, and more detailed deductions can be made regarding the basic factors that influence degeneration and regeneration in the OS.

In the mouse OS, the olfactotoxin methyl bromide was used to eliminate functional ORN inputs to the OB. Responses recovered after lesion to near-normal levels of magnitude within 12 weeks, although some evidence of mistargeting of the regenerated ORN axons onto OB targets was found. This shows how the OS has extensive ability in reestablishing connections to the CNS, and indicates that the mechanisms mediating ORN targeting during bulbar reinnervation throughout developmental stages remain active after development is complete, and allow sensory representations to be greatly restored after massive ORN loss. Other studies have

reported on the regenerative capacity and glomerular convergence of specific ORN populations, and shown that odor memories are conserved after ORN lesion and recovery (Schwob et al., 1999; Costanzo, 2000; Cummings et al., 2000; St. John and Key, 2003; McMillan Carr et al., 2004; Blanco-Hernández et al., 2012). The mechanisms underlying the reestablishment of topography are not yet fully elucidated, but may include axonal guidance cues (Schwob, 2002; Schwarting and Henion, 2011), olfactory receptor identity (Feinstein et al., 2004) and the ORN cell type (Bozza et al., 2009). The number of ORNs surviving the lesion seems to be related to the degree of mistargeting after recovery (Schwob et al., 1999). Retargeting of certain specific ORN populations to their appropriate glomerulus was found to be normal if only these neurons were selectively lesioned (Gogos et al., 2000). Also, a higher target precision was observed for ORNs recovered after chemical lesions that spared the lamina propria (Blanco-Hernández et al., 2012). Altogether, results indicate that the ability of the OE to recover and reestablish functional inputs to the OB persists even after extreme peripheral damage, but is dependent on the extent of this damage.

Recovery of function in the OS of larval *X. laevis* was observed after transection of the ON. Nonetheless, metamorphosis is eminent and extensive regeneration of the OS may seem unnecessary, as the whole system will soon be completely reorganized. Since recovery was observed, this indicates that olfaction in larval *X. laevis* may be of great importance to survival. Or more interestingly, the function of the OS in larval *X. laevis* may somehow be relevant to or influence function of the OS after metamorphosis, in the adult frog. Although during metamorphosis the gradual reorganization of the OS involves the replacement of most ORNs and substantial rewiring, the OS never loses its capacity to process olfactory information.

The OS of larval *X. laevis* seems to recover morphologically and functionally 6-7 weeks after unilateral transection of the ON. This recovery is apparently quite extensive and function is restored, but it would be interesting to see what alterations occur after lesion, at a more detailed level. Once the spatiotemporal odor evoked map has been established for larval *X. laevis*, under normal conditions, a comparison with altered models subjected to different forms of lesion will be possible, and more detailed deductions can be made regarding the basic factors that influence degeneration and regeneration in the OS. Once the odor map is well established for *Xenopus*, it can be used as control to compare to odor evoked maps of animals that have recovered

olfactory function after lesion. This will allow us to functionally characterize the short and long-term effects different lesions have on this system. Knowing in detail how the OB responds to different stimulus, and how these responses are altered after injury, will allow a clearer view of how the brain recovers after lesion.

## REFERENCES

Altman, J. (1969). Autoradiographic and histological studies of postnatal neurogenesis. IV. Cell proliferation and migration in the anterior forebrain, with special reference to persisting neurogenesis in the olfactory bulb. *Journal of Comparative Neurology*, 137(4), 433-457.

Altman, J. & Das, G. D. (1965). Autoradiographic and histological evidence of postnatal hippocampal neurogenesis in rats. *The Journal of Comparative Neurology*, 124(3), 319-335.

Altner, H. (1962). Untersuchungen über Leistungen und Bau der Nase des südafrikanischen Krallenfrosches *Xenopus laevis* (Daudin, 1803). *Zeitschrift für vergleichende Physiologie*, 45(3), 272-306.

Ankarcrona, M., Dypbukt, J. M., Bonfoco, E., Zhivotovsky, B., Orrenius, S., Lipton, S. A., & Nicotera, P. (1995). Glutamate-induced neuronal death: a succession of necrosis or apoptosis depending on mitochondrial function. *Neuron*, 15(4), 961-973.

Archiga, H. & Alcocer-Cuaron, C. (1969). Adrenergic effects on electro-olfactogram. *Experimental Medicine and Surgery*, 27(4), 384.

Bauer, S., Rasika, S., Han, J., Mauduit, C., Raccurt, M., Morel, G., Jourdan, F., Benahmed, M., Moyse, E., Patterson, P. H. (2003). Leukemia inhibitory factor is a key signal for injury-induced neurogenesis in the adult mouse olfactory epithelium. *The Journal of Neuroscience*, 23(5), 1792-1803.

Beal, M. F. (1995). Aging, energy, and oxidative stress in neurodegenerative diseases. *Annals of Neurology*, 38(3), 357-366.

Beites, C. L., Kawauchi, S., Crocker, C. E., & Calof, A. L. (2005). Identification and molecular regulation of neural stem cells in the olfactory epithelium. *Experimental Cell Research*, 306(2), 309-316.

Bergman, U., Östergren, A., Gustafson, A. L., & Brittebo, E. (2002). Differential effects of olfactory toxicants on olfactory regeneration. *Archives of Toxicology*, 76(2), 104-112.

Bergström, U., Giovanetti, A., Piras, E., & Brittebo, E. B. (2003). Methimazole-induced damage in the olfactory mucosa: effects on ultrastructure and glutathione levels. *Toxicologic Pathology*, 31(4), 379-387.

Bernocchi, G., Scherini, E., Giacometti, S., Mares, V. (1990). Premitotic DNA synthesis in the brain of the adult frog (*Rana esculenta L.*): an autoradiographic 3H-thymidine study. *The Anatomical Record*, 228, 461–470.

Betarbet, R., Zigova, T., Bakay, R. A., Luskin, M. B. (1996). Dopaminergic and GABAergic interneurons of the olfactory bulb are derived from the neonatal subventricular zone. *International Journal of Developmental Neuroscience*, 14, 921–930.

Blanco-Hernández, E., Valle-Leija, P., Zomosa-Signoret, V., Drucker-Colín, R. & Vidaltamayo, R. (2012). Odor memory stability after reinnervation of the olfactory bulb. *PLoS ONE*, 7(10), e46338.

Bouvet, J. F., Delaleu, J. C. & Holley, A. (1988). The activity of olfactory receptor cells is affected by acetylcholine and substance P. *Neuroscience Research*, 5(3), 214-223.

Bozza, T., Vassalli, A., Fuss, S., Zhang, J. J., Weiland, B., Pacifico, R., Feinstein, P., & Mombaerts, P. (2009). Mapping of class I and class II odorant receptors to glomerular domains by two distinct types of olfactory sensory neurons in the mouse. *Neuron*, 61(2), 220-233.

Bracey, N. A., Beck, P. L., Muruve, D. A., Hirota, S. A., Guo, J., Jabagi, H., Wright, J. R., & Duff, H. J. (2013). The Nlrp3 inflammasome promotes myocardial dysfunction in structural cardiomyopathy through interleukin-1 $\beta$ . *Experimental Physiology*, 98(2), 462-472.

Brandstätter, R., Kotrschal, K. (1990). Brain growth patterns in four European cyprinid fish species (*Cyprinidae, Teleostei*): roach (*Rutilus rutilus*), bream (*Abramis brama*), common carp (*Cyprinus carpio*) and sabre carp (*Pelecus cultratus*). *Brain, Behavior and Evolution*, 35,195–211.

Breer, H., Fleischer, J. & Strotmann, J. (2006). The sense of smell: multiple olfactory subsystems. *Cellular and Molecular Life Sciences*, 63(13), 1465-1475.

Brenner, C. & Moulin, M. (2012). Physiological roles of the permeability transition pore. *Circulation research*, *111*(9), 1237-1247.

Brockes, J. P. (1997). Amphibian limb regeneration: rebuilding a complex structure. *Science*, *276*(5309), 81-87.

Brockes, J. P. & Kumar, A. (2002). Plasticity and reprogramming of differentiated cells in amphibian regeneration. *Nature Reviews Molecular Cell Biology*, *3*(8), 566-574.

Buckland, M. E. & Cunningham, A. M. (1998). Alterations in the neurotrophic factors BDNF, GDNF and CNTF in the regenerating olfactory system. *Annals of the New York Academy of Sciences*, *855*(1), 260-265.

Burd, C. G., Matunis, E. L. & Dreyfuss, G. I. D. E. O. N. (1991). The multiple RNA-binding domains of the mRNA poly (A)-binding protein have different RNA-binding activities. *Molecular and Cellular Biology*, *11*(7), 3419-3424.

Burnstock, G. (2007). Physiology and pathophysiology of purinergic neurotransmission. *Physiological Reviews*, *87*(2), 659-797.

Byrd, C. A. & Brunjes, P. C. (1995). Organization of the olfactory system in the adult zebrafish: histological, immunohistochemical, and quantitative analysis. *Journal of Comparative Neurology*, *358*(2), 247-259.

Byrd, C. A. & Burd, G. D. (1991). Development of the olfactory bulb in the clawed frog, *Xenopus laevis*: a morphological and quantitative analysis. *Journal of Comparative Neurology*, *314*(1), 79-90.

Cai, J., Yang, J. & Jones, D. (1998). Mitochondrial control of apoptosis: the role of cytochrome c. *Biochimica et Biophysica Acta (BBA)-Bioenergetics*, *1366*(1), 139-149.

Calof, A. L., Mumm, J. S., Rim, P. C., & Shou, J. (1998). The neuronal stem cell of the olfactory epithelium. *Journal of Neurobiology*, *36*(2), 190-205.

Càmara, C. G., & Harding, J. W. (1984). Thymidine Incorporation in the olfactory epithelium of mice: Early exponential response induced by olfactory neurectomy. *Brain Research*, *308*(1), 63-68.



Cameron, H. A., Woolley, C. S., McEwen, B. S., Gould, E. (1993). Differentiation of newly born neurons and glia in the dentate gyrus of the adult rat. *Neuroscience*, 56:337–344

Carleton, A., Petreanu, L. T., Lansford, R., Alvarez-Buylla, A., Lledo, P. M. (2003). Becoming a new neuron in the adult olfactory bulb. *Nature. Neuroscience*, 6,507–518.

Carr, V. M., & Farbman, A. I. (1992). Ablation of the olfactory bulb up-regulates the rate of neurogenesis and induces precocious cell death in olfactory epithelium. *Experimental Neurology*, 115(1), 55-59.

Carter, L. A., MacDonald, J. L., & Roskams, A. J. (2004). Olfactory horizontal basal cells demonstrate a conserved multipotent progenitor phenotype. *The Journal of Neuroscience*, 24(25), 5670-5683.

Caviness, V. S., Takahashi, T., & Nowakowski, R. S. (1995). Numbers, time and neocortical neuronogenesis: a general developmental and evolutionary model. *Trends in Neurosciences*, 18(9), 379-383.

Chao, T. I., Kasa, P., & Wolff, J. R. (1997). Distribution of astroglia in glomeruli of the rat main olfactory bulb: exclusion from the sensory subcompartment of neuropil. *Journal of Comparative Neurology*, 388(2), 191-210.

Chen, T. W., Lin, B. J., & Schild, D. (2009). Odor coding by modules of coherent mitral/tufted cells in the vertebrate olfactory bulb. *Proceedings of the National Academy of Sciences*, 106(7), 2401-2406.

Chess, A., Simon, I., Cedar, H., & Axel, R. (1994). Allelic inactivation regulates olfactory receptor gene expression. *Cell*, 78(5), 823-834.

Chetverukhin, V. K., Polenov, A. L. (1993). Ultrastructural radioautographic analysis of neurogenesis in the hypothalamus of the adult frog, *Rana temporaria*, with special reference to physiological regeneration of the preoptic nucleus. I. Ventricular zone cell proliferation. *Cell Tissue Research*, 271, 341–350.

Cheung, E. C., Melanson-Drapeau, L., Cregan, S. P., Vanderluit, J. L., Ferguson, K. L., McIntosh, W. C., Park, D. S., Bennett, S. A. L. & Slack, R. S. (2005). Apoptosis-

inducing factor is a key factor in neuronal cell death propagated by BAX-dependent and BAX-independent mechanisms. *The Journal of Neuroscience*, 25(6), 1324-1334.

Cheung, M. C., Jang, W., Schwob, J. E., & Wachowiak, M. (2013). Functional recovery of odor representations in regenerated sensory inputs to the olfactory bulb. *Frontiers in Neural Circuits*, 7, 207.

Christensen, M. D., Holbrook, E. H., Costanzo, R. M., & Schwob, J. E. (2001). Rhinotomy is disrupted during the re-innervation of the olfactory bulb that follows transection of the olfactory nerve. *Chemical Senses*, 26(4), 359-369.

Christie, K. J., Turbic, A., & Turnley, A. M. (2013). Adult hippocampal neurogenesis, Rho kinase inhibition and enhancement of neuronal survival. *Neuroscience*, 247, 75-83.

Coleman, M. L., Sahai, E. A., Yeo, M., Bosch, M., Dewar, A., & Olson, M. F. (2001). Membrane blebbing during apoptosis results from caspase-mediated activation of ROCK I. *Nature cell biology*, 3(4), 339-345.

Costanzo, R. M. (2000). Rewiring the olfactory bulb: changes in odor maps following recovery from nerve transection. *Chemical Senses*, 25(2), 199-205.

Costanzo, R. M., & Graziadei, P. P. (1983). A quantitative analysis of changes in the olfactory epithelium following bulbectomy in hamster. *Journal of Comparative Neurology*, 215(4), 370-381.

Cowan, C. M., Thai, J., Krajewski, S., Reed, J. C., Nicholson, D. W., Kaufmann, S. H., & Roskams, A. J. (2001). Caspases 3 and 9 send a pro-apoptotic signal from synapse to cell body in olfactory receptor neurons. *The Journal of Neuroscience*, 21(18), 7099-7109.

Cummings, D. M., Emge, D. K., Small, S. L., & Margolis, F. L. (2000). Pattern of olfactory bulb innervation returns after recovery from reversible peripheral deafferentation. *Journal of Comparative Neurology*, 421(3), 362-373.

Cummings, D. M., Henning, H. E., & Brunjes, P. C. (1997). Olfactory bulb recovery after early sensory deprivation. *The Journal of Neuroscience*, 17(19), 7433-7440.

Czesnik, D., Kuduz, J., Schild, D., & Manzini, I. (2006). ATP activates both receptor and sustentacular supporting cells in the olfactory epithelium of *Xenopus laevis* tadpoles. *European Journal of Neuroscience*, *23*(1), 119-128.

Czesnik, D., Schild, D., Kuduz, J., & Manzini, I. (2007). Cannabinoid action in the olfactory epithelium. *Proceedings of the National Academy of Sciences*, *104*(8), 2967-2972.

Dawley, E. M., Fingerlin, A., Hwang, D., John, S. S., Stankiewicz, C. A. (2000). Seasonal cell proliferation in the chemosensory epithelium and brain of red-backed salamanders, *Plethodon cinereus*. *Brain, Behavior and Evolution*, *56*, 1–13.

DeHamer, M. K., Guevara, J. L., Hannon, K., Olwin, B. B., & Calof, A. L. (1994). Genesis of olfactory receptor neurons in vitro: regulation of progenitor cell divisions by fibroblast growth factors. *Neuron*, *13*(5), 1083-1097.

Delay, R. J., & Dionne, V. E. (2002). Two second messengers mediate amino acid responses in olfactory sensory neurons of the salamander, *Necturus maculosus*. *Chemical Senses*, *27*(8), 673-680.

Dittrich, K., Kuttler, J., Hassenklöver, T., & Manzini, I. (2015). Metamorphic remodeling of the olfactory organ of the African clawed frog, *Xenopus laevis*. *Journal of Comparative Neurology*, in press.

Doetsch, F., Scharff, C. (2001). Challenges for brain repair: insights from adult neurogenesis in birds and mammals. *Brain, Behavior and Evolution*, *58*:306–322

Doty, R. L. (1979). A review of olfactory dysfunctions in man. *American Journal of Otolaryngology*, *1*(1), 57-79.

Duan, S., Anderson, C. M., Stein, B. A., & Swanson, R. A. (1999). Glutamate induces rapid upregulation of astrocyte glutamate transport and cell-surface expression of GLAST. *The Journal of Neuroscience*, *19*(23), 10193-10200.

Eisthen, H. L., Delay, R. J., Wirsig-Wiechmann, C. R., & Dionne, V. E. (2000). Neuromodulatory effects of gonadotropin releasing hormone on olfactory receptor neurons. *The Journal of Neuroscience*, *20*(11), 3947-3955.

Eriksson, P. S., Perfilieva, E., Bjork-Eriksson, T., Alborn, A. M., Nordborg, C., Peterson, D. A., Gage, F.H. (1998). Neurogenesis in the adult human hippocampus. *Nature Medicine*, 4, 1313–1317.

Evans, H. E.(1952). The correlation of brain pattern and feeding habits in four species of cyprinid fishes. *Journal of Comparative Neurology*, 97, 133–142.

Farbman, A. I. (1990). Olfactory neurogenesis: genetic or environmental controls? *Trends in Neurosciences*, 13(9), 362-365.

Farbman, A. I., & Buchholz, J. A. (1996). Transforming growth factor- $\alpha$  and other growth factors stimulate cell division in olfactory epithelium in vitro. *Journal of Neurobiology*, 30(2), 267-280.

Faulkner, R. L., Wishard, T. J., Thompson, C. K., Liu, H. H., & Cline, H. T. (2015). FMRP Regulates Neurogenesis in Vivo in *Xenopus Laevis* Tadpoles. *Eneuro*, 2(1), ENEURO-0055.

Feinstein, P., Bozza, T., Rodriguez, I., Vassalli, A., & Mombaerts, P. (2004). Axon guidance of mouse olfactory sensory neurons by odorant receptors and the  $\beta$ 2 adrenergic receptor. *Cell*, 117(6), 833-846.

Féron, F., Vincent, A., & Mackay-Sim, A. (1999). Dopamine promotes differentiation of olfactory neuron in vitro. *Brain Research*, 845(2), 252-259.

Ferretti, P. (2004). Neural stem cell plasticity: recruitment of endogenous populations for regeneration. *Current Neurovascular Research*, 1, 215–229.

Filoni, S., & Gibertini, G. (1969). A study of the regenerative capacity of the central nervous system of anuran amphibia in relation to their stage of development. I. Observations on the regeneration of the optic lobe of *Xenopus laevis* (Daudin) in the larval stages. *Archives de Biologie*, 80(4), 369.

Filoni S, Gibertini G. (1971). A study of the regeneration of the cerebellum of *Xenopus leavis* (Daudin) in the larval stages and after metamorphosis. *Archives of Biology*, 82, 433–470.

Font, E., Desfilis, E., Pérez-Cañellas, M. M., & Garcia-Verdugo, J. M. (2001). Neurogenesis and neuronal regeneration in the adult reptilian brain. *Brain, Behavior and Evolution*, 58(5), 276-295.

Föske, H. (1934). Das Geruchsorgan von *Xenopus laevis*. *Anatomy and Embryology*, 103(5), 519-550.

Freitag, J., Krieger, J., Strotmann, J., & Breer, H. (1995). Two classes of olfactory receptors in *Xenopus laevis*. *Neuron*, 15(6), 1383-1392.

Fritz, A., Gorlick, D. L., & Burd, G. D. (1996). Neurogenesis in the olfactory bulb of the frog *Xenopus laevis* shows unique patterns during embryonic development and metamorphosis. *International Journal of Developmental Neuroscience*, 14(7), 931-943.

Gage, F. H. (2000). Mammalian neural stem cells. *Science*, 287(5457), 1433-1438.

Garcia-Verdugo, J. M., Ferron, S., Flames, N., Collado, L., Desfilis, E., Font, E. (2002). The proliferative ventricular zone in adult vertebrates: a comparative study using reptiles, birds, and mammals. *Brain Research Bulletin*, 57, 765-775.

Glazner, G. W., Camandola, S., & Mattson, M. P. (2000). Nuclear factor- $\kappa$ B mediates the cell survival-promoting action of activity-dependent neurotrophic factor peptide-9. *Journal of Neurochemistry*, 75(1), 101-108.

Gliem, S., Syed, A. S., Sansone, A., Kludt, E., Tantalaki, E., Hassenklöver, T., Korsching, S. I., & Manzini, I. (2013). Bimodal processing of olfactory information in an amphibian nose: odor responses segregate into a medial and a lateral stream. *Cellular and Molecular Life Sciences*, 70(11), 1965-1984.

Gogos, J. A., Osborne, J., Nemes, A., Mendelsohn, M., & Axel, R. (2000). Genetic ablation and restoration of the olfactory topographic map. *Cell*, 103(4), 609-620.

Gordon, M. K., Mumm, J. S., Davis, R. A., Holcomb, J. D., & Calof, A. L. (1995). Dynamics of MASH1 expression in vitro and in vivo suggest a non-stem cell

site of MASH1 action in the olfactory receptor neuron lineage. *Molecular and Cellular Neuroscience*, 6(4), 363-379.

Graziadei, P. P. C. (1971). Topological relations between olfactory neurons. *Zeitschrift für Zellforschung und Mikroskopische Anatomie*, 118(4), 449-466.

Graziadei, P. P. C. (1973). Cell dynamics in the olfactory mucosa. *Tissue and Cell*, 5(1), 113-131.

Graziadei, P. P. C., & Graziadei, G. M. (1978). Continuous nerve cell renewal in the olfactory system. In *Development of Sensory Systems* (pp. 55-83). Springer Berlin Heidelberg.

Graziadei, P. P. C., & Graziadei, G. M. (1979). Neurogenesis and neuron regeneration in the olfactory system of mammals. I. Morphological aspects of differentiation and structural organization of the olfactory sensory neurons. *Journal of Neurocytology*, 8(1), 1-18.

Graziadei, P. P. C., & Metcalf, J. F. (1971). Autoradiographic and ultrastructural observations on the frog's olfactory mucosa. *Zeitschrift für Zellforschung und Mikroskopische Anatomie*, 116(3), 305-318.

Greenlund, L. J., Deckwerth, T. L., & Johnson, E. M. (1995). Superoxide dismutase delays neuronal apoptosis: a role for reactive oxygen species in programmed neuronal death. *Neuron*, 14(2), 303-315.

Haas, K., Jensen, K., Sin, W. C., Foa, L., & Cline, H. T. (2002). Targeted electroporation in *Xenopus* tadpoles in vivo—from single cells to the entire brain. *Differentiation*, 70(4-5), 148-154.

Hagg, T., Varon, S., & Louis, J. C. (1993). Ciliary neurotrophic factor (CNTF) promotes low-affinity nerve growth factor receptor and CD4 expression by rat CNS microglia. *Journal of Neuroimmunology*, 48(2), 177-187.

Halbach, O. V. B. (2007). Immunohistological markers for staging neurogenesis in adult hippocampus. *Cell and Tissue Research*, 329 (3), 409-420.

Hansen, A., Reiss, J. O., Gentry, C. L., & Burd, G. D. (1998). Ultrastructure of the olfactory organ in the clawed frog, *Xenopus laevis*, during larval development and metamorphosis. *Journal of Comparative Neurology*, *398*, 273-288.

Hansen, A., Rolen, S. H., Anderson, K., Morita, Y., Caprio, J., & Finger, T. E. (2003). Correlation between olfactory receptor cell type and function in the channel catfish. *The Journal of Neuroscience*, *23*(28), 9328-9339.

Harding, J. W., Getchell, T. V., & Margolis, F. L. (1978). Denervation of the primary olfactory pathway in mice. V. Long-term effect of intranasal ZnSO<sub>4</sub> irrigation on behavior, biochemistry and morphology. *Brain Research*, *140*(2), 271-285.

Hassenklöver, T., & Manzini, I. (2013). Olfactory wiring logic in amphibians challenges the basic assumptions of the unbranched axon concept. *The Journal of Neuroscience*, *33*(44), 17247-17252.

Hassenklöver, T., & Manzini, I. (2014). The olfactory system as a model to study axonal growth patterns and morphology in vivo. *Journal of Visualized Experiments* (92), e52143.

Hassenklöver, T., Kurtanska, S., Bartoszek, I., Junek, S., Schild, D., & Manzini, I. (2008). Nucleotide-induced Ca<sup>2+</sup> signaling in sustentacular supporting cells of the olfactory epithelium. *Glia*, *56*(15), 1614-1624.

Hassenklöver, T., Schwartz, P., Schild, D., & Manzini, I. (2009). Purinergic signaling regulates cell proliferation of olfactory epithelium progenitors. *Stem Cells*, *27*(8), 2022-2031.

Hastings, N. B., Gould, E. (1999). Rapid extension of axons into the CA3 region by adult-generated granule cells. *Journal of Comparative Neurology*, *413*:146–54

Hegg, C. C., & Lucero, M. T. (2004). Dopamine reduces odor-and elevated-K<sup>+</sup>-induced calcium responses in mouse olfactory receptor neurons in situ. *Journal of Neurophysiology*, *91*(4), 1492-1499.

Hegg, C. C., Au, E., Roskams, A. J., & Lucero, M. T. (2003). PACAP is present in the olfactory system and evokes calcium transients in olfactory receptor neurons. *Journal of Neurophysiology*, *90*(4), 2711-2719.

Hegg, C., Doherty, J., Crudgington, S., & Jones, E. (2008). ATP induces proliferation and neuroprotection in Swiss Webster mouse olfactory epithelium. *The FASEB Journal*, 22 (Meeting Abstract Supplement), 59.6.

Higgs, D. M., & Burd, G. D. (2001). Neuronal turnover in the *Xenopus laevis* olfactory epithelium during metamorphosis. *Journal of Comparative Neurology*, 433(1), 124-130.

Howell, B. J., Baumgardner, F. W., Bondi, K., & Rahn, H. (1970). Acid-base balance in cold-blooded vertebrates as a function of body temperature. *American Journal of Physiology-Legacy Content*, 218(2), 600-606.

Huard, J. M., Youngentob, S. L., Goldstein, B. J., Luskin, M. B., & Schwob, J. E. (1998). Adult olfactory epithelium contains multipotent progenitors that give rise to neurons and non-neural cells. *Journal of Comparative Neurology*, 400(4), 469-486.

Junek, S., Chen, T. W., Alevra, M., & Schild, D. (2009). Activity correlation imaging: visualizing function and structure of neuronal populations. *Biophysical Journal*, 96(9), 3801-3809.

Kasowski, H. J., Kim, H., & Greer, C. A. (1999). Compartmental organization of the olfactory bulb glomerulus. *Journal of Comparative Neurology*, 407(2), 261-274.

Kauffman, S. L. (1968). Lengthening of the generation cycle during embryonic differentiation of the mouse neural tube. *Experimental cell research*, 49(2), 420-424.

Kawai, F., Kurahashi, T., & Kaneko, A. (1999). Adrenaline enhances odorant contrast by modulating signal encoding in olfactory receptor cells. *Nature Neuroscience*, 2(2), 133-138.

Kirsche, W. (1967). On postembryonic matrix zones in the brain of various vertebrates and their relationship to the study of the brain structure. *Zeitschrift für Mikroskopisch-Anatomische Forschung*, 77, 313-406.

Kirsche, W. (1950). Die regenerativen Vorgänge am Rückenmark erwachsener Teleostier nach operativer Kontinuitätstrennung. *Zeitschrift für Mikroskopisch-Anatomische Forschung*, 56, 190-265.



Kirsche, W. (1960). Experimentelle Untersuchungen zur Frage der Regeneration und Function des Tectum opticum von *Carassius carassius*. *Zeitschrift für Mikroskopisch-Anatomische Forschung*, 67, 140–182.

Kirsche, W. (1965). Regenerative processes in the brain and spinal cord. *Ergebnisse der Anatomie und Entwicklungsgeschichte*, 38, 143-194.

Kempermann, G., Wiskott, L., Gage, F. H. (2004). Functional significance of adult neurogenesis. *Current Opinion in Neurobiology*, 14, 186–191.

Kerr, M. A., & Belluscio, L. (2006). Olfactory experience accelerates glomerular refinement in the mammalian olfactory bulb. *Nature Neuroscience*, 9(4), 484-486.

Liu, X., Kim, C. N., Yang, J., Jemmerson, R., & Wang, X. (1996). Induction of apoptotic program in cell-free extracts: requirement for dATP and cytochrome c. *Cell*, 86(1), 147-157.

Lois, C., Alvarez-Buylla, A. (1994). Long-distance neuronal migration in the adult mammalian brain. *Science*, 264, 1145–1148.

López-García, C., Tineo, P. L., & Del Corral, J. (1984). Increase of the neuron number in some cerebral cortical areas of a lizard, *Podarcis hispanica*, (Steind., 1870), during postnatal periods of life. *Journal für Hirnforschung*, 25(3), 255-259.

Luskin, M. B. (1993). Restricted proliferation and migration of postnatally generated neurons derived from the forebrain subventricular zone. *Neuron*, 11, 173–189.

Ma, L., & Michel, W. C. (1998). Drugs affecting phospholipase C-mediated signal transduction block the olfactory cyclic nucleotide-gated current of adult zebrafish. *Journal of Neurophysiology*, 79(3), 1183-1192.

Ma, M. (2007). Encoding olfactory signals via multiple chemosensory systems. *Critical Reviews in Biochemistry and Molecular Biology*, 42(6), 463-480.

Malnic, B., Hirono, J., Sato, T., & Buck, L. B. (1999). Combinatorial receptor codes for odors. *Cell*, 96(5), 713-723.

Manzini, I. (2015). From neurogenesis to neuronal regeneration: the amphibian olfactory system as a model to visualize neuronal development in vivo. *Neural Regeneration Research*, 10(6), 872-874.

Manzini, I., & Schild, D. (2003). cAMP-independent olfactory transduction of amino acids in *Xenopus laevis* tadpoles. *The Journal of Physiology*, 551(1), 115-123.

Manzini, I., & Schild, D. (2004). Classes and narrowing selectivity of olfactory receptor neurons of *Xenopus laevis* tadpoles. *The Journal of General Physiology*, 123(2), 99-107.

Manzini, I., Brase, C., Chen, T. W., & Schild, D. (2007a). Response profiles to amino acid odorants of olfactory glomeruli in larval *Xenopus laevis*. *The Journal of Physiology*, 581(2), 567-579.

Manzini, I., Heermann, S., Czesnik, D., Brase, C., Schild, D., & Rössler, W. (2007b). Presynaptic protein distribution and odour mapping in glomeruli of the olfactory bulb of *Xenopus laevis* tadpoles. *European Journal of Neuroscience*, 26(4), 925-934.

Manzini, I., Rössler, W., & Schild, D. (2002). cAMP-independent responses of olfactory neurons in *Xenopus laevis* tadpoles and their projection onto olfactory bulb neurons. *The Journal of Physiology*, 545(2), 475-484.

Marcus, R. C., Delaney, C. L., Easter, S. S., Jr. (1999). Neurogenesis in the visual system of embryonic and adult zebrafish (*Danio rerio*). *Visual Neuroscience*, 16, 417-424.

Martínez-Guijarro, F. J., Blasco-Ibáñez, J. M., & Freund, T. F. (1994). Serotonergic innervation of nonprincipal cells in the cerebral cortex of the lizard *Podarcis hispanica*. *Journal of Comparative Neurology*, 343(4), 542-553.

Mattson, M. P. (2007). Calcium and neurodegeneration. *Aging cell*, 6(3), 337-350.

Mattson, M. P., Barger, S. W., Furukawa, K., Bruce, A. J., Wyss-Coray, T., Mark, R. J., & Mucke, L. (1997). Cellular signaling roles of TGF $\beta$ , TNF $\alpha$  and  $\beta$ APP in brain injury responses and Alzheimer's disease. *Brain Research Reviews*, 23(1), 47-61.

Mattson, M. P., Culmsee, C., & Yu, Z. F. (2000). Apoptotic and antiapoptotic mechanisms in stroke. *Cell and Tissue Research*, 301(1), 173-187.

Mattson, M. P., Keller, J. N., & Begley, J. G. (1998). Evidence for synaptic apoptosis. *Experimental Neurology*, 153(1), 35-48.

McCurdy, R. D., Féron, F., McGrath, J. J., & Mackay-Sim, A. (2005). Regulation of adult olfactory neurogenesis by insulin-like growth factor-I. *European Journal of Neuroscience*, 22(7), 1581-1588.

McKay, S. E., Purcell, A. L., & Carew, T. J. (1999). Regulation of synaptic function by neurotrophic factors in vertebrates and invertebrates: implications for development and learning. *Learning & Memory*, 6(3), 193-215.

McMillan Carr, V., Ring, G., Youngentob, S. L., Schwob, J. E., & Farbman, A. I. (2004). Altered epithelial density and expansion of bulbar projections of a discrete HSP70 immunoreactive subpopulation of rat olfactory receptor neurons in reconstituting olfactory epithelium following exposure to methyl bromide. *Journal of Comparative Neurology*, 469(4), 475-493.

Mehler, M. F., Mabie, P. C., Zhu, G., Gokhan, S., & Kessler, J. A. (2000). Developmental changes in progenitor cell responsiveness to bone morphogenetic proteins differentially modulate progressive CNS lineage fate. *Developmental Neuroscience*, 22(1-2), 74-85.

Meisami, E., Mikhail, L., Baim, D., & Bhatnagar, K. P. (1998). Human olfactory bulb: aging of glomeruli and mitral cells and a search for the accessory olfactory bulba. *Annals of the New York Academy of Sciences*, 855(1), 708-715.

Menini, A. (Ed.). (2009). *The Neurobiology of Olfaction*. CRC Press.

Mezler, M., Konzelmann, S., Freitag, J., Rossler, P., & Breer, H. (1999). Expression of olfactory receptors during development in *Xenopus laevis*. *The Journal of Experimental Biology*, 202(4), 365-376.

Middleton, G., Hamanoue, M., Enokido, Y., Wyatt, S., Pennica, D., Jaffray, E., Hay, R. T., & Davies, A. M. (2000). Cytokine-induced nuclear factor kappa B

activation promotes the survival of developing neurons. *The Journal of Cell Biology*, 148(2), 325-332.

Mombaerts, P. (2004). Odorant receptor gene choice in olfactory sensory neurons: the one receptor–one neuron hypothesis revisited. *Current Opinion in Neurobiology*, 14(1), 31-36.

Mombaerts, P. (2006). Axonal wiring in the mouse olfactory system. *Annual Review in Cell and Developmental Biology*, 22, 713-737.

Mombaerts, P., Wang, F., Dulac, C., Chao, S. K., Nemes, A., Mendelsohn, M., Edmondson, J. & Axel, R. (1996). Visualizing an olfactory sensory map. *Cell*, 87(4), 675-686.

Mori, K., & Sakano, H. (2011). How is the olfactory map formed and interpreted in the mammalian brain? *Annual Review of Neuroscience*, 34, 467-499.

Morrison, S. J. (2001). Neuronal potential and lineage determination by neural stem cells. *Current Opinion in Cell Biology*, 13(6), 666-672.

Moulton, D. G. (1974). Dynamics of cell populations in the olfactory epithelium. *Annals of the New York Academy of Sciences*, 237(1), 52-61.

Moulton, D. G., Celebi, G., & Fink, R. P. (1970). Olfaction in mammals—two aspects: proliferation of cells in the olfactory epithelium and sensitivity to odours. In *Ciba Foundation Symposium-Taste and Smell in Vertebrates* (pp. 227-250). John Wiley & Sons, Ltd.

Mousley, A., Polese, G., Marks, N. J., & Eisthen, H. L. (2006). Terminal nerve-derived neuropeptide  $\gamma$  modulates physiological responses in the olfactory epithelium of hungry axolotls (*Ambystoma mexicanum*). *The Journal of Neuroscience*, 26(29), 7707-7717.

Murdoch, B., & Roskams, A. J. (2007). Olfactory epithelium progenitors: insights from transgenic mice and in vitro biology. *Journal of Molecular Histology*, 38(6), 581-599.

Nakatani, H., Serizawa, S., Nakajima, M., Imai, T., & Sakano, H. (2003). Developmental elimination of ectopic projection sites for the transgenic OR gene that

has lost zone specificity in the olfactory epithelium. *European Journal of Neuroscience*, 18(9), 2425-2432.

Nef, P., Hermans-Borgmeyer, I., Artieres-Pin, H., Beasley, L., Dionne, V. E., & Heinemann, S. F. (1992). Spatial pattern of receptor expression in the olfactory epithelium. *Proceedings of the National Academy of Sciences*, 89(19), 8948-8952.

Nezlin, L. P., & Schild, D. (2000). Structure of the olfactory bulb in tadpoles of *Xenopus laevis*. *Cell and Tissue Research*, 302(1), 21-29.

Nezlin, L. P., & Schild, D. (2005). Individual olfactory sensory neurons project into more than one glomerulus in *Xenopus laevis* tadpole olfactory bulb. *Journal of Comparative Neurology*, 481(3), 233-239.

Nezlin, L. P., Heermann, S., Schild, D., & Rössler, W. (2003). Organization of glomeruli in the main olfactory bulb of *Xenopus laevis* tadpoles. *Journal of Comparative Neurology*, 464(3), 257-268.

Nieuwkoop, P. D., & Faber, J. (1994). Normal Table of *Xenopus laevis* (Daudin) Garland Publishing Inc. New York, London.

Niimura, Y., & Nei, M. (2005). Evolutionary dynamics of olfactory receptor genes in fishes and tetrapods. *Proceedings of the National Academy of Sciences*, 102(17), 6039-6044.

Oppenheim, R. W. (1991). Cell death during development of the nervous system. *Annual Review of Neuroscience*, 14(1), 453-501.

Petti, M. A., Matheson, S. F., & Burd, G. D. (1999). Differential antigen expression during metamorphosis in the tripartite olfactory system of the African clawed frog, *Xenopus laevis*. *Cell and Tissue Research*, 297(3), 383-396.

Pinching, A. J., & Powell, T. P. S. (1971). The neuropil of the glomeruli of the olfactory bulb. *Journal of Cell Science*, 9(2), 347-377.

Platel, R. (1974). Poids encéphalique et indice d'encéphalisation chez les reptiles sauriens. *Zoologischer Anzeiger*, 192(5-6), 332-382.

Polenov, A. L., Chetverukhin, V. K. (1993). Ultrastructural radioautographic analysis of neurogenesis in the hypothalamus of the adult frog, *Rana temporaria*, with special reference to physiological regeneration of the preoptic nucleus. II. Types of neuronal cells produced. *Cell Tissue Research*, 271:351–362

Raucci, F., Di Fiore, M. M., Pinelli, C., D'Aniello, B., Luongo, L., Polese, G., Rastogi, R. K. (2006). Proliferative activity in the frog brain: a PCNA-immunohistochemistry analysis. *Journal of Chemical Neuroanatomy*, 32:127–142.

Reiss, J. O., & Burd, G. D. (1997a, April). Cellular and molecular interactions in the development of the *Xenopus* olfactory system. In *Seminars in Cell & Developmental Biology* (Vol. 8, No. 2, pp. 171-179). Academic Press.

Reiss, J. O., & Burd, G. D. (1997b). Metamorphic remodeling of the primary olfactory projection in *Xenopus*: developmental independence of projections from olfactory neuron subclasses. *Journal of Neurobiology*, 32(2), 213-222.

Ressler, K. J., Sullivan, S. L., & Buck, L. B. (1993). A zonal organization of odorant receptor gene expression in the olfactory epithelium. *Cell*, 73(3), 597-609.

Ressler, K. J., Sullivan, S. L., & Buck, L. B. (1994). Information coding in the olfactory system: evidence for a stereotyped and highly organized epitope map in the olfactory bulb. *Cell*, 79(7), 1245-1255.

Richter, W. (1965). Regeneration in the tectum opticum of *Leucaspius delineatus* (Heckel 1843). *Zeitschrift für Mikroskopisch-Anatomische Forschung*. 74, 46–68.

Richter, W. (1969). Regeneration im Telencephalon von juvenilen und adulten *Lebistes reticulatus* (Teleostei). *Zeitschrift für Mikroskopisch-Anatomische Forschung*, 81, 345–358.

Richter, W., Kranz, D. (1981). Autoradiographische Untersuchungen der postnatalen Proliferationsaktivität der Matrixzonen des Gehirns der Forelle (*Salmo irideus*). *Zeitschrift für Mikroskopisch-Anatomische Forschung*, 95, 491–520.

Roskams, A. J., Bethel, M. A., Hurt, K. J., & Ronnett, G. V. (1996). Sequential expression of Trks A, B, and C in the regenerating olfactory neuroepithelium. *The Journal of Neuroscience*, *16*(4), 1294-1307.

Saraiva, L. R., & Korsching, S. I. (2007). A novel olfactory receptor gene family in teleost fish. *Genome Research*, *17*(10), 1448-1457.

Sastry, P. S., & Rao, K. S. (2000). Apoptosis and the nervous system. *Journal of Neurochemistry*, *74*(1), 1-20.

Schild, D. (1985). A computer-controlled device for the application of odours to aquatic animals. *Journal of Electrophysiological Techniques*, *12*(2), 71-79.

Schoppa, N. E., & Westbrook, G. L. (2001). Glomerulus-specific synchronization of mitral cells in the olfactory bulb. *Neuron*, *31*(4), 639-651.

Schwartz, G. A., & Henion, T. R. (2011). Regulation and function of axon guidance and adhesion molecules during olfactory map formation. *Journal of Cellular Biochemistry*, *112*(10), 2663-2671.

Schwob, J. E. (1992). The biochemistry of olfactory neurons: stages of differentiation and neuronal subsets. In *Science of Olfaction* (pp. 80-125). Springer New York.

Schwob, J. E. (2002). Neural regeneration and the peripheral olfactory system. *The Anatomical Record*, *269*(1), 33-49.

Schwob, J. E., Youngentob, S. L., & Mezza, R. C. (1995). Reconstitution of the rat olfactory epithelium after methyl bromide-induced lesion. *Journal of Comparative Neurology*, *359*(1), 15-37.

Schwob, J. E., Youngentob, S. L., Ring, G., Iwema, C. L., & Mezza, R. C. (1999). Reinnervation of the rat olfactory bulb after methyl bromide-induced lesion: Timing and extent of reinnervation. *Journal of Comparative Neurology*, *412*(3), 439-457.

Segaar J. (1965). Behavioural aspects of degeneration and regeneration in fish brain: a comparison with higher vertebrates. *Progress and Brain Research*, *14*, 143-231.

Seri, B., Garcia-Verdugo, J. M., McEwen, B. S., Alvarez-Buylla, A. (2001). Astrocytes give rise to new neurons in the adult mammalian hippocampus. *The Journal of Neuroscience*, 21, 7153–7160.

Seri, B., Garcia-Verdugo, J.M., Collado-Morente, L., McEwen, B. S., Alvarez-Buylla, A. (2004). Cell types, lineage, and architecture of the germinal zone in the adult dentate gyrus. *Journal of Comparative Neurology*, 478, 359–378.

Shi, P., & Zhang, J. (2007). Comparative genomic analysis identifies an evolutionary shift of vomeronasal receptor gene repertoires in the vertebrate transition from water to land. *Genome research*, 17(2), 166-174.

Shou, J., Rim, P. C., & Calof, A. L. (1999). BMPs inhibit neurogenesis by a mechanism involving degradation of a transcription factor. *Nature Neuroscience*, 2(4), 339-345.

Shou, Y., Gunasekar, P. G., Borowitz, J. L., & Isom, G. E. (2000). Cyanide-induced apoptosis involves oxidative-stress-activated NF- $\kappa$ B in cortical neurons. *Toxicology and Applied Pharmacology*, 164(2), 196-205.

Sibbing, W. (1953). Postnatale Regeneration der verschiedenen Hirnabschnitte bei Urodelen. *Development Genes and Evolution*, 146(4), 433-486.

Simpson, P. J., Wang, E., Moon, C., Matarazzo, V., Cohen, D. R., Liebl, D. J., & Ronnett, G. V. (2003). Neurotrophin-3 signaling maintains maturational homeostasis between neuronal populations in the olfactory epithelium. *Molecular and Cellular Neuroscience*, 24(4), 858-874.

Slack, J. M., Beck, C. W., Gargioli, C., Christen, B. (2004). Cellular and molecular mechanisms of regeneration in *Xenopus*. *Philosophical Transactions of the Royal Society B*. 359, 745–751.

Slee, E. A., Adrain, C., & Martin, S. J. (1999). Serial killers: ordering caspase activation events in apoptosis. *Cell Death and Differentiation*, 6(11), 1067-1074.

Srebro, Z. (1965). Endbrain regeneration in adult *Xenopus laevis*. *Folia Biologica*, 13(3), 269-280.



St John, J. A., & Key, B. (2003). Axon mis-targeting in the olfactory bulb during regeneration of olfactory neuroepithelium. *Chemical Senses*, 28(9), 773-779.

Strotmann, J., Wanner, I., Krieger, J., Raming, K., & Breer, H. (1992). Expression of odorant receptors in spatially restricted subsets of chemosensory neurones. *Neuroreport*, 3(12), 1053-1056.

Sulz, L., & Bacigalupo, J. (2006). Role of nitric oxide during neurogenesis in the olfactory epithelium. *Biological Research*, 39(4), 589-599.

Tamatani, M., Ogawa, S., & Tohyama, M. (1998). Roles of Bcl-2 and caspases in hypoxia-induced neuronal cell death: a possible neuroprotective mechanism of peptide growth factors. *Molecular Brain Research*, 58(1), 27-39.

Thompson, C. K., & Brenowitz, E. A. (2010). Neuroprotective effects of testosterone in a naturally occurring model of neurodegeneration in the adult avian song control system. *Journal of Comparative Neurology*, 518(23), 4760-4770.

Thorne, P. R., & Housley, G. D. (1996, August). Purinergic signalling in sensory systems. In *Seminars in Neuroscience* (Vol. 8, No. 4, pp. 233-246). Academic Press.

Tseng, A. S., Adams, D. S., Qiu, D., Koustubhan, P., & Levin, M. (2007). Apoptosis is required during early stages of tail regeneration in *Xenopus laevis*. *Developmental Biology*, 301(1), 62-69.

Vargas, G., & Lucero, M. T. (1999). Dopamine modulates inwardly rectifying hyperpolarization-activated current ( $I_h$ ) in cultured rat olfactory receptor neurons. *Journal of Neurophysiology*, 81(1), 149-158.

Vassar, R., Chao, S. K., Sitcheran, R., Nun, J. M., Vosshall, L. B., & Axel, R. (1994). Topographic organization of sensory projections to the olfactory bulb. *Cell*, 79(6), 981-991.

Vassar, R., Ngai, J., & Axel, R. (1993). Spatial segregation of odorant receptor expression in the mammalian olfactory epithelium. *Cell*, 74(2), 309-318.

Vedin, V., Slotnick, B., & Berghard, A. (2004). Zonal ablation of the olfactory sensory neuroepithelium of the mouse: effects on odorant detection. *European Journal of Neuroscience*, 20(7), 1858-1864.

Watt, F. M. (2001). Stem cell fate and patterning in mammalian epidermis. *Current Opinion in Genetics & Development*, *11*(4), 410-417.

Weiler, E., & Farbman, A. I. (1997). Proliferation in the rat olfactory epithelium: age-dependent changes. *The Journal of Neuroscience*, *17*(10), 3610-3622.

Wu, H. H., Ivkovic, S., Murray, R. C., Jaramillo, S., Lyons, K. M., Johnson, J. E., & Calof, A. L. (2003). Autoregulation of neurogenesis by GDF11. *Neuron*, *37*(2), 197-207.

Yee, K. K., & Costanzo, R. M. (1998). Changes in odor quality discrimination following recovery from olfactory nerve transection. *Chemical Senses*, *23*(5), 513-519.

Yoshino, J., & Tochinai, S. (2004). Successful reconstitution of the non-regenerating adult telencephalon by cell transplantation in *Xenopus laevis*. *Development, Growth & Differentiation*, *46*(6), 523-534.

Yoshino, J., & Tochinai, S. (2006). Functional regeneration of the olfactory bulb requires reconnection to the olfactory nerve in *Xenopus* larvae. *Development, Growth & Differentiation*, *48*(1), 15-24.

Yuan, J., & Yankner, B. A. (2000). Apoptosis in the nervous system. *Nature*, *407*(6805), 802-809.

Zou, D. J., Feinstein, P., Rivers, A. L., Mathews, G. A., Kim, A., Greer, C. A., Mombaerts, P., & Firestein, S. (2004). Postnatal refinement of peripheral olfactory projections. *Science*, *304*(5679), 1976-1979.

Zupanc, G. K. (2001). Adult neurogenesis and neuronal regeneration in the central nervous system of teleost fish. *Brain, Behavior and Evolution*, *58*, 250-275.